NASA-TM-87642 19860015957

NASA Technical Memorandum 87642

Mass Spectrometric Gas Composition Measurements Associated With Jet Interaction Tests in a High-Enthalpy Wind Tunnel

Beverley W. Lewis, Kenneth G. Brown,
George M. Wood, Jr., Richard L. Puster,
Patricia A. Paulin, Charles E. Fishel,
and D. Alan Ellerbe

LIBRARY COPY

LANGLEY RESEARCH CENTER
LIBRARY, NASA
HAMPTON, VIRGINIA

JUNE 1986

NASA

NASA Technical Memorandum 87642

Mass Spectrometric Gas Composition Measurements Associated With Jet Interaction Tests in a High-Enthalpy Wind Tunnel

Beverley W. Lewis
Langley Research Center
Hampton, Virginia

Charles E. Fishel
Old Dominion University
Norfolk, Virginia

Kenneth G. Brown
Old Dominion University
Norfolk, Virginia

D. Alan Ellerbe
Langley Research Center
Hampton, Virginia

George M. Wood, Jr., Richard L. Puster, and Patricia A. Paulin
Langley Research Center
Hampton, Virginia

National Aeronautics and Space Administration

Scientific and Technical Information Branch

1986

Summary

The need for determining gas composition is becoming increasingly important in wind-tunnel experiments to measure aerothermodynamic interactions. Mass spectrometric (MS) techniques are in development at Langley Research Center. This paper describes measurements made by continuously sampling at the top of the test section during test runs of the Langley 7-Inch High-Temperature Tunnel. The tests were performed to investigate the extent of mixing of an inert gas injected into the test stream from a jet on a flat-plate model and to monitor the combustion products resulting from the ignition of a high-pressure mixture of natural gas and air. The MS measurement yields the mole fraction of inert gas species (neon or helium) which reached the top of the test section as well as the carbon dioxide (CO_2) from the tunnel combustion gas test stream. The data, obtained under a variety of tunnel run conditions, are related to the pressures measured in the test section of the tunnel and the pressures measured at the gold-leak inlet of the MS. The apparent distributions of the injected gas species and tunnel gas (CO_2) are discussed in terms of the sampling technique with and without the use of an inert tracer.

Introduction

Mass spectrometric analyses were conducted in the Langley 7-Inch High-Temperature Tunnel (7-Inch HTT). The tests conducted during the analyses were designed to study the interaction of an underexpanded Mach 2.2 jet of gas that was injected from the surface of a flat plate with the hypersonic, high-enthalpy test stream. (See fig. 1(a).) The test stream is formed as a result of the high-pressure combustion of a mixture of natural gas and air expanded through a contoured conical nozzle. The tests were conducted to investigate the resultant flow field and heat distribution within the test section. They were designed to assess the need for protective measures if tests were made with high-temperature jet injections and to determine the incidence of tunnel "unstarting" due to the flow-field disturbances caused by the jet gas injection.

The mass spectrometric measurements were made during the tests to satisfy the following objectives: (1) to determine the concentration of the injected gas which reached the top of the hemispherically shaped test section, and (2) to determine the concentration of carbon dioxide (CO_2) which reached the top of the test section. Both were to be measured as they changed during the operational sequence of the tunnel runs. There were several variations in test conditions as follows: (1) hot and cold test-stream runs, (2) model in and out of the stream with jet firing, and (3) jet gas either a 1 mole percent Neon in Nitrogen (1 mole percent Ne/N_2) mixture or pure helium (He). The test conditions for each run discussed in this paper are listed in table I.

The general objective was to improve the understanding and interpretation of mass spectrometric data obtained in the dynamic and hostile environment of a high-enthalpy wind tunnel. The supersonic-jet interaction experiments described in this report are one part of an integrated investigation which includes laboratory experiments and theoretical and modeling studies of sampling integrity in severe dynamic environments. Any effect of sample inlet and gas transfer system (probe and tubing) on the composition of the sample is of prime importance, since the desired measurement is the local composition just outside the sampling inlet or probe.

Symbols

I_i	peak-height intensity measured by mass spectrometer, Hz (may be converted to amperes by factor of 10^{-13} A/Hz)
J ON	jet turned on
J OFF	jet turned off
MI	model inserted in test stream
MO	model withdrawn from test stream
P_i	partial pressure of ith species, torr
P_{gl}	total pressure at gold-leak inlet of MS, torr
P_{ts}	total pressure in test section, torr
P_{tg}	partial pressure of tunnel gas, torr
S_i	MS sensitivity of ith species, Hz/torr
X_i	mole fraction of ith species
Subscripts:	
i, j	ith and jth species
msd	measured
nom	nominal
Abbreviations:	
C	cold tunnel run
H	hot tunnel run
JO	jet on
MS	mass spectrometer
MV	manual valve

SV	solenoid-operated valve
7-Inch HTT	Langley 7-Inch High-Temperature Tunnel

Experimental Methods

Tunnel Test Conditions

The tests were conducted in the Langley 7-Inch High-Temperature Tunnel (7-Inch HTT). The gas was injected into the test stream from a nozzle opening in the surface of a flat-plate wedge model. (See fig. 1(a).) The model was mounted on a retractable sting at an angle of attack of $-8°$, and the flush jet nozzle was inclined forward at an angle of 15° from the normal to the flat-plate surface. Figure 1(b) is a typical shadowgraph of the flow over the model with the gas injection during a test run. Figure 2 is a schematic of the sampling system. The nominal tunnel hot run conditions were as follows: Mach 7 with an approximate stagnation pressure of 2200 psia and a temperature of 3360°R. Jet chamber pressures were varied from 20 to 135 psia. Table I gives pertinent run conditions for the runs whose data are given and discussed in this paper.

Mass Spectrometric Sampling and Measurements

In these experiments, the sampling inlets (fig. 1(a)) were located at the top of the test section to determine the amount of injected gas that escaped from the tunnel test stream. All inlets were located in a line coplanar with the centerline of the test stream, and only one inlet was open during a run. The rake at inlet B could be rotated 180° to increase the number of sampling points with respect to the flat plate shown in figure 1(a). The inlets on the rake were opened or closed with threaded plugs and were approximately 1/4 in. in diameter. The inlet was designed to minimize any possible sampling effects. The sampled flow was quiescent, and the temperature of sampled gas was near ambient; therefore, the gases measured were inert or unreactive under these conditions. The 10 ft of 1/4-in. outside-diameter copper-tubing transfer line connecting the inlet to the MS has been shown in laboratory studies to have minimal effect upon the sample composition. (See ref. 1.) Sampling integrity was thus considered to be good in these tests.

The simplest view of the test situation is that the injected gas mixes with the stream gas and diffuses from the stream boundary as a constant composition mixture. The gas then displaces and/or mixes with the gas in the test section and is sampled at the top of the test section. The final mixture of the gases of interest is not further changed when it is transported to the mass spectrometer (MS). For purposes of this study, effects of pumping on flow about the inlet orifice and the species-dependent differences in flow from within the stream to the inlet, although undefined, were assumed to be negligible.

The MS used was a gas analysis and detection system (GADS) that contained a small portable hyperbolic-rod quadrupole mass analyzer. A microcomputer provided control, data acquisition, calibration, quantitative analysis, and housekeeping functions. The GADS instrument is described in references 2 and 3. An automated analysis mode provides for the monitoring of up to 40 mass peaks in the range of 2 to 200 atomic mass units (amu) by peak stepping. For this study, 2 or 3 mass peaks were monitored with a cycle time of 0.3 second for 3 peaks; therefore, a peak-height intensity measurement was recorded every 0.1 second. Test runs were typically on the order of 1 to 2 minutes overall. The model was typically in the test section about 3 seconds for hot runs and up to 11 seconds for cold runs. The injection jet was on for about 2.5 seconds for hot runs and up to 10 seconds for cold runs. The quadrupole MS was located adjacent to the tunnel test section and was remotely operated from the tunnel control room by a duplicate keyboard and an analog oscilloscope monitor. MS data were digitally stored for subsequent printout.

To distinguish between nitrogen injected into the stream and the relatively large amount of nitrogen present in the methane-air combustion products, 1 mole percent neon was added as a tracer to the injected gas. In subsequent tests, the injected gas was pure He, which is inert and can be sampled and measured directly. The GADS had been previously calibrated in the laboratory for sensitivity to Ne, He, Ar, and CO_2 using pure gases and standard mixtures of these gases with air. When the jet gas was 1 mole percent Ne/N_2, the peaks monitored were Ne at 20 amu, Ar at 40 amu, and, after a number of runs, CO_2 at 44 amu. When He was the jet gas, He at 4 amu, Ar at 40 amu, and CO_2 at 44 amu were monitored. As is discussed subsequently, the Ar 40 peak was used as an internal standard for both cases.

Dividing the intensity of the MS peak of a particular molecular species by the intensity of the MS peak of a species of known concentration which remains chemically unchanged by the combustion process yields quantitative information about the composition of the mixture. In combustion processes, the MS peak at 40 amu, due to the inert gas Ar present in the original fuel-air mixture, provides a convenient and easily identifiable reference. Since the reference gas is present in the original combus-

tor mixture, all the physical processes which occur in the combustor and at the nozzle should affect I_{Ar} and all other species relatively. Dividing the peak intensity of a combustion product, such as CO_2, by that of Ar should then eliminate most of the interference and reduce the pressure-dependent uncertainty in the measurement. Therefore, any observed change in I_{CO_2}/I_{Ar} from the nominal value must be the result of some physical or chemical change occurring in the combustor, nozzle, test stream, or sampling system that affects the CO_2 concentration. If one of the gases being ratioed to Ar does not originate in the combustor (gases injected from the flat-plate model), some of the combustor-nozzle physical processes may be superimposed upon the ratio and can be measured.

Intensity ratios are also used with other tracers of known composition, such as the Ne in the N_2 jet gas used in these studies. Here, I_{Ne}/I_{Ar} is an effective ratio of the gas injection to combustion process and is used to trace the mixing of the jet gas with the combustion test gas at the top of the test section. This ratio uses the assumed constant concentration of Ar in the tunnel test gas and the constant concentration of Ne in the N_2 jet gas to indicate a changing mixture ratio of jet gas to tunnel gas during a tunnel run. This ratio can be made quantitative by applying calibrated sensitivity factors S_i which relate peak-height intensity to partial pressure of the appropriate species. Thus, the mixing ratio of the 1 mole percent Ne/N_2 jet gas with hot tunnel gas is given by

$$\frac{P_{N_2,jet}}{P_{tg}} = \left(\frac{I_{Ne}}{I_{Ar}}\right)\left(\frac{S_{Ar}}{S_{Ne}}\right)\left(\frac{0.86}{1.00}\right)$$

where

S_{Ar} $= 5.64 \times 10^4$ Hz/torr

S_{Ne} $= 6.82 \times 10^4$ Hz/torr

0.86 = Mole percent Ar in tunnel gas

1.00 = Mole percent Ne in jet gas

For cold tunnel gas runs (standard dry air),

$$\frac{P_{N_2,jet}}{P_{Air}} = \left(\frac{I_{Ne}}{I_{Ar}}\right)\left(\frac{S_{Ar}}{S_{Ne}}\right)\left(\frac{0.93}{1.00}\right)$$

where 0.93 = Mole percent Ar in standard dry air. When He is the jet gas, the equations are as follows:

$$\frac{P_{He,jet}}{P_{tg}} = \left(\frac{I_{He}}{I_{Ar}}\right)\left(\frac{S_{Ar}}{S_{He}}\right)\left(\frac{0.86}{100}\right)$$

(Hot tunnel gas condition runs)

and

$$\frac{P_{He,jet}}{P_{Air}} = \left(\frac{I_{He}}{I_{Ar}}\right)\left(\frac{S_{Ar}}{S_{He}}\right)\left(\frac{0.93}{100}\right)$$

(Cold tunnel gas condition runs)

In these equations, $S_{He} = 1.37 \times 10^6$ Hz/torr, and the jet gas is 100 mole percent He. The use of He as the jet gas allows a more direct measurement, since it is itself a single inert gas that is directly determined by mass spectrometry. Figures 3 through 7 show the model position (height) and typical run test-section and gold-leak pressure traces for five different test conditions. (See table I.) These figures also show that the pressure measured with a differential capacitance transducer at the gold-leak (P_{gl}), inlet of the MS followed sensibly the pressure changes in the pod (P_{ts}), although they were attenuated as was expected. In most of these tests, the pressure rise caused by the insertion of the model can be separated from the pressure rise caused by the firing of the jet in the model. In general, the pressure rise when the jet was fired was slightly larger than when the model was inserted for both the test-section and the gold-leak inlet locations.

Examples of the changes in the measured intensities and derived data during the course of two different test runs are shown in figures 8 through 13 for test runs 72 and 91. Figures 8 and 9 show the MS peak-height intensity I_i curves in Hertz (10^{-13} amp/Hz) for neon (I_{Ne}), helium (I_{He}), argon (I_{Ar}), and carbon dioxide (I_{CO_2}). They also show the gold-leak pressure P_{gl} and the derived ratios of I_{Ne} to I_{Ar} or I_{He} to I_{Ar}. The nominal static mixing ratio of 0.035 for jet-to-tunnel gases is given for comparison. From the intensity data and MS sensitivity S_i calibration data, the partial pressures P_i of Ne, He, Ar, and CO_2 were calculated using the equation $P_i = I_i/S_i$, where S_i is in Hertz/torr. Figures 10 and 11 give the partial pressures of interest and the P_{gl}. From the partial pressures and the total pressure of the sample at the gold-leak P_{gl}, the mole fraction X_i can be calculated by the equation $X_i = P_i/P_{gl}$. The mole fractions are shown in figures 12 and 13. The intensity curves of figures 8 and 9 and the partial-pressure curves of figures 10 and 11 have similar shapes for a given species in a particular run. However, the mole-fraction curves of figures 12 and 13 have shapes that differ from the I_i and P_i curves. The intensity-ratio

curves in figures 8 and 9 also have partially different shapes than the I_i and P_i curves. The I_i and P_i similarities are the result of their dependence on the number density of the species, which is independent of other species present. The mole-fraction curve X_i is dependent on the total number density of the gas mixture. The ratio I_i/I_j is relative to number densities of components i and j of a gas mixture.

Results and Discussion

Jet Gas Interaction

Figures 14 through 21 summarize and compare the data taken for test runs where the tunnel and instruments were operating in nominal fashion. (See table I for run conditions.) Figure 14 shows the variation of I_{Ar} with time for hot and cold runs where the 1 mole percent Ne/N_2 jet was fired before or at the same time the model was inserted in the test stream. For the hot runs, I_{Ar} peaked during the time the model with jet firing was in the test stream and then decreased until the model was withdrawn and the jet was stopped. For the cold runs, I_{Ar} increased rapidly at first and then approached a constant level during the time the model with jet firing was in the stream. The I_{Ar} trends and the difference in average peak intensity (about 5×10^2 greater in the hot runs) indicate that there was a difference in the mixing and migration of the tunnel test gas to the top of the test section between the hot and cold test streams.

Figure 15 shows I_{Ar} curves for hot and cold runs with He as the jet gas and with the jet fired about 0.5 second after the model insertion. For these hot runs, the I_{Ar} increased as the model was inserted; I_{Ar} reached a maximum when the jet fired and dropped sharply just after the model was withdrawn and the jet was stopped. In the cold runs, I_{Ar} increased with model insertion and approached a plateau that lasted until the model was withdrawn. Cold-run curves did not include model withdrawal and jet stopping data. The Ar intensities measured for both the hot and cold runs with He jet were at about the same level.

The changes in mole fraction X_i for the N_2 jet gas and the He jet gas with time are shown in figures 16 and 17; X_{Ne} and X_{He} were obtained from the MS peak intensity data sampled from the top of the test section. The He jet runs of figure 17 show similar trends with a decrease in He background as the model was inserted, a large, sharp rise in X_{He} as the jet was fired, and a slow decrease until the model was withdrawn and the jet was turned off. Differences between hot and cold runs were presumed to be due to differences in the pumping of the flows. In the case of the N_2 jet (fig. 16), the same trends are evident (as in fig. 17) but are not as well defined. The peaking of X_{Ne} after the jet is fired is shown, as is the decrease while the model was inserted with jet firing. The N_2 jet runs differed from most of the He jet runs in that the jet was fired before, or at the same time that, the model was inserted; for the He runs, the jet was fired after the model was in the test stream.

Figures 18 and 19 show I_{Ne}/I_{Ar} and I_{He}/I_{Ar} for cold and hot runs, respectively. For the cold runs, the curves show a peaking of the intensity ratios while the jet was firing and then a decrease until the model was removed and the jet was stopped. For the hot runs with the He jet, the intensity-ratio curves tended to increase sharply when the jet was fired and either peaked or leveled off before the model was retracted. In figure 19, the peaking was more pronounced when the jet gas was N_2, than for He. This observation may be the result of greater diffusion rates.

Figure 20 shows the percentage of N_2 jet gas that was measured at the top of the test section during several runs. When the N_2 jet gas was injected into the hot test stream, the jet gas increased in the sample to a maximum and then decreased somewhat before the model was withdrawn and the jet was turned off. Most of the runs produced gas mixtures with between 50 and 80 mole percent jet N_2 at the top. One cold run (27) with the jet fired below the test stream is also shown. The N_2 jet gas at the top of the test section reached 60 mole percent, indicating that there was little mixing or entrainment of jet gas with the test stream under these conditions.

In figure 21 (He jet gas runs), all the runs except run 91 had mixtures of He and tunnel gas at the top which were less than 1 mole percent He. Run 91 was one in which the He jet was fired below the hot test stream and produced a gas mixture at the top of the test section. This mixture had a He concentration of about 55 mole percent, which shows that most of the He ejected from the jet traveled around the test stream to the top with minimal interaction with the test stream. The fact that He did not show up at the test-section top in any concentrations greater than 1 mole percent when injected into a hot or cold test stream indicates that most of the He was entrained with those test streams and was removed from the test section.

When a N_2 jet is injected into a hot or cold stream, the injected gas mixes with the test-stream gas and diffuses to the top of the test section as a mixture. When a N_2 jet is fired below a cold stream, there is only slight mixing with the test-stream gas, and apparently much of the jet N_2 gas goes directly to the top of the test section and passes around the test stream. Helium behaved the same way when fired below a hot stream. From these results, it is suggested that the molecular weight differences

between the injected gas and the test-stream gas produce significant differences in stream mixing and diffusion from the stream. Nitrogen with a molecular weight of 28 is similar to air (79 mole percent N_2) with an average molecular weight of 29 that mixes and diffuses at similar rates. Helium with a molecular weight of 4 appears to be mainly entrained in the test stream and does not diffuse out readily nor is it picked up from outside the hot stream.

Carbon Dioxide Distribution

Carbon dioxide (CO_2) differs from the other gases measured in these tests in that CO_2 is a product of the combustion reaction of methane (CH_4) and oxygen (O_2). The CO_2 levels will serve, then, as a monitor of the overall combustion-system efficiency. The other gases measured, Ne, He, and Ar, are all chemically inert and were introduced at constant concentration levels in the jet gas or were already present in the tunnel gas. Of the inert gases in the test section, only Ar had any concentration dependence on the combustion process, and then only if the fuel-to-air ratio changed. During a test run in which the combustor performed stably and according to the nominal conditions of fuel-to-air ratio which is 8:10 stoichiometric to CO_2 and water (H_2O), the mole ratio of CO_2 to Ar should remain constant at 8.7 if there are no physical or chemical processes taking place in the system which remove CO_2 from the hot test gas stream or sample stream. The mole ratio of 8.7 corresponds to a measured intensity ratio I_{CO_2}/I_{Ar} of 3.5 for the GADS in these tests. These are theoretical maximum stream values assuming complete combustion and equilibrium flow. With a cold-gas stream, the CO_2 concentration would be on the order of 0.03 mole percent (average atmospheric value), the mole ratio of CO_2 to Ar would be 0.03, and I_{CO_2}/I_{Ar} would be 0.014. We, however, were measuring at the top of the test section and were testing the assumption that the gases that reach this sampling point arrive without significant change in concentration or composition from average stream values except for mixing. With these considerations in mind, the CO_2 data are presented and discussed in the paragraphs that follow.

Figure 22 shows MS peak-height intensity data for CO_2 and Ar for a hot run (86) with He jet firing in the test stream. In figure 22(a), three intensity curves are shown—Ar peak intensity, CO_2 intensity, and nominal CO_2 intensity—calculated from I_{Ar} and the nominal I_{CO_2}/I_{Ar} ratio for the combustion-gas test-stream value of 3.5. In figure 22(b), two intensity-ratio curves are shown, $(I_{CO_2}/I_{Ar})_{msd}$ and $(I_{CO_2}/I_{Ar})_{nom}$. The latter is a constant-value straight line at 3.5. The shapes of the I_i curves are reasonable and show that the measured I_{CO_2} curve is similar to the nominal I_{CO_2} curve, although it is attenuated by about 24 percent at the peak of the curves. Some dilution (I_i attenuation) of the test-stream gas is expected because of the jet gas injected and because of the mixing with gases already in the top of the test section.

Figures 23 through 26 show curves of the measured I_{CO_2} and I_{Ar} and the nominal I_{CO_2} and $(I_{CO_2}/I_{Ar})_{msd}$ as a function of time for four runs each as labeled. The agreement between the runs is good considering the complexity of the systems involved. Figures 23, 24, and 26 also show averaged measured curves (dotted lines) for these four runs. They display the trend of an increase in CO_2 intensity as the "model-in" period is approached, peaking toward the end of jet injection and dropping sharply just before the "model-out" and "jet-off" events.

Figure 27 shows curves of P_{gl}, I_{CO_2}, and X_{CO_2} for 3 different types of runs with He jet injection, cold and hot runs with model in and jet on (figs. 27(a) and 27(c)), and a hot run with model out and jet fired beneath the test stream (fig. 27(b)). In the cold run (fig. 27(a)), the measured CO_2 level was about 0.04 mole percent (compared with ambient air at 0.03 mole percent) and was somewhat oscillatory over the larger run time. The hot run with the jet fired below the test stream (fig. 27(b)) showed a drop in CO_2 concentration from about 3.6 mole percent to about 1.2 mole percent when the He jet was fired. This indicates that a large amount of the ejected He migrated directly to the top of the test section and diluted the CO_2 (tunnel test gas) by a little more than 1:1. (See fig. 21.) Figure 27(c), where the He was injected into the hot test stream, shows the X_{CO_2} peaking before the model was inserted and then generally decreasing as the jet was firing, until the model was withdrawn and the jet was shut off, after which it increased and peaked again. This trend, shown in the curves in figure 28, indicates that dilution or removal of CO_2 from the top of the test section is faster than diffusion from the test stream during the model-in, "jet-on" part of the run. The shapes of the curves in figure 28 are determined by the change of P_{CO_2}/P_{gl} with time during a run. In this case, there is a relatively constant P_{CO_2} with an increasing P_{gl} that peaks as the model is withdrawn and as the jet is turned off. The pressures, P_{CO_2} and P_{gl}, are determined by the rate at which CO_2 diffuses from the test stream to the top of the test section with other test-stream and jet gas components. Changes in P_{gl} are the result of He jet addition and subsequent diffusion to the top of the test section. This includes any effects that the injection may have on the diffusion of all the other

species present. The MS inlet pressure P_{gl} is directly related to the test-section pressure P_{ts} but is smaller because of the pressure drop through the 10-ft-long transfer line.

Figure 28 shows the mole fraction of CO_2 plotted against time for a number of hot runs. The same trend was observed when the model was in the test stream for all runs shown, including one where the jet was fired with the model below the test stream. The trend was for the X_{CO_2} to decrease during the test interval, which was about 3 seconds for these hot runs. The trend is in agreement with the assumption that CO_2 and other hot stream gases diffuse to the top of the test section. During the 2.5-second jet firing the test gases are diluted by and/or displaced by a mixture of jet gas and test-stream gas of decreased CO_2 content. For longer runs it would be expected to level off to a steady state, however, longer runs at this combustion temperature and pressure were not feasible in the 7-Inch HTT. Another factor which could affect the CO_2 concentration, which has not been previously discussed in this paper, is the real possibility of the formation of water droplets which can dissolve CO_2 and effectively remove it from the gaseous phase.

The results indicate that some previous boundary-layer CO_2 meaurements from inlets on a conical model in the Langley 8-Foot High-Temperature Tunnel (ref. 4) have qualitative validity and, under more controlled measurement conditions, may be capable of quantitation.

Concluding Remarks

The mass spectrometric measurements made during the supersonic jet interaction tests in the Langley 7-Inch High-Temperature Tunnel provided significant information of a semiquantitative nature concerning the real-time distribution of the injected gases in the test section. The measurements of CO_2 and Ar diffusing to the top of the test section under several tunnel run conditions gave indications of the stability of the combustion gas test-stream composition. The quantitative aspects of the CO_2 measurements were well within reasonable ranges of nominal operating values. Laboratory tests indicate that the sampling system was performing well for the gas conditions being sampled; that is, there were low flow rates at the sample port, ambient temperature at the test-section wall, and out-of-stream test-section pressure in the range of 15 to 31 torr.

NASA Langley Research Center
Hampton, VA 23665-5225
February 7, 1986

References

1. Brown, K. G.: *Analysis of an Effusive Sampling Device for Analysis of Boundary Layer Gases.* NAS1-17099, Old Dominion Univ., Oct. 1983. (Available as NASA CR-174532.)
2. Wood, G. M.; and Yeager, P. R.: A Computer-Controlled Quadrupole Mass Spectrometer for Automated Environmental Analysis. *Environmental and Climatic Impact of Coal Utilization,* Jag J. Singh and Adarsh Deepak, eds., Academic Press, Inc., 1980, pp. 187–211.
3. Judson, Charles M.; Josias, Conrad; and Lawrence, James L., Jr.: *Design and Fabrication of a Basic Mass Analyzer and Vacuum System.* NASA CR-2815, 1977.
4. Wood, George M., Jr.; Lewis, Beverley W.; Upchurch, Billy T.; Nowak, Robert J.; Eide, Donald G.; and Paulin, Patricia A.: Developing Mass Spectrometric Techniques for Boundary Layer Measurement in Hypersonic High Enthalpy Test Facilities. *ICIASF '83 Record,* IEEE Publ. 83CH1954-7, IEEE, 1983, pp. 259–270.

TABLE I. TUNNEL RUN CONDITIONS

Run	Jet		Model position	Sample port	Time, sec	
	Gas	Pressure, psia			MI	Jet on
27 (cold)	Ne/N_2	50	MO	A	0	3.6
28 (hot)	Ne/N_2	50	MI	A	2.4	2.4
31 (hot)	Ne/N_2	50	MI	A	2.4	2.4
47 (hot)	Ne/N_2	70	MI	B1	2.6	2.6
49 (hot)	Ne/Ne	70	MI	B1	3.0	3.0
59 (cold)	Ne/N_2	135	MI	B1	7.0	7.0
60 (cold)	Ne/N_2	70	MI	B1	4.6	4.6
61 (cold)	Ne/N_2	135	MI	B1	4.2	4.2
72 (hot)	Ne/N_2	67	MI	B1	3.8	3.8
85 (hot)	He	20	MI	B1	3.0	2.3
86 (hot)	He	20	MI	B1	3.2	2.3
88 (hot)	He	55	MI	B3	2.6	2.2
89 (hot)	He	62	MI	B3	3.2	2.4
91 (hot)	He	62	MO	B2	0	6.1
93 (hot)	Jet off	Jet off	MI	[a]B2	1.2	0
96a (cold)	He	61	MI	[a]B2	11.6	10.8
96b (cold)	He	61	MI	[a]B2	11.2	10.6

[a]Sample arm rotated 180°.

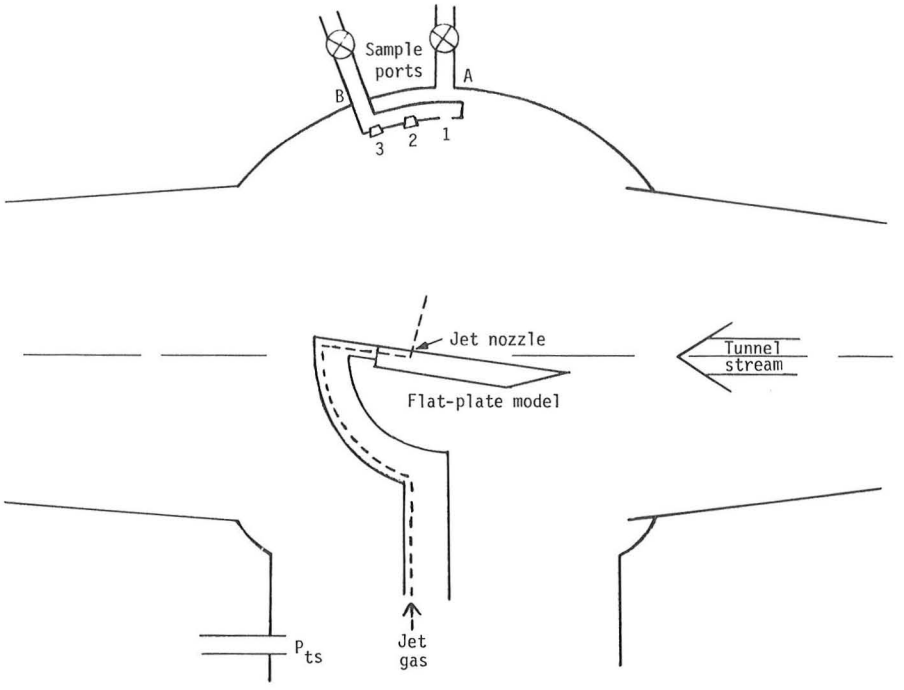

(a) Flat-plate model with thruster jet nozzle angled 15° forward in plate surface as mounted in 7-Inch HTT.

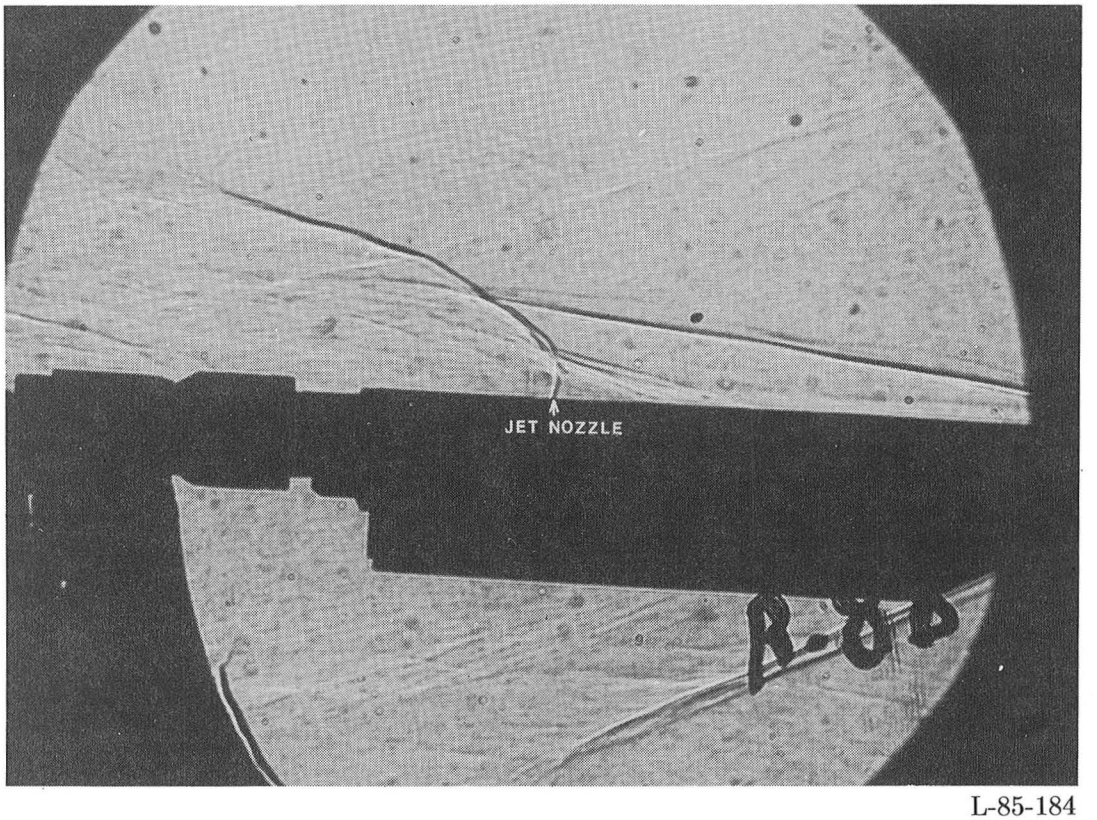

L-85-184

(b) Shadowgraph of flat-plate model in hot test stream with helium injection from plate showing typical flow patterns.

Figure 1. Flat-plate model in 7-Inch HTT.

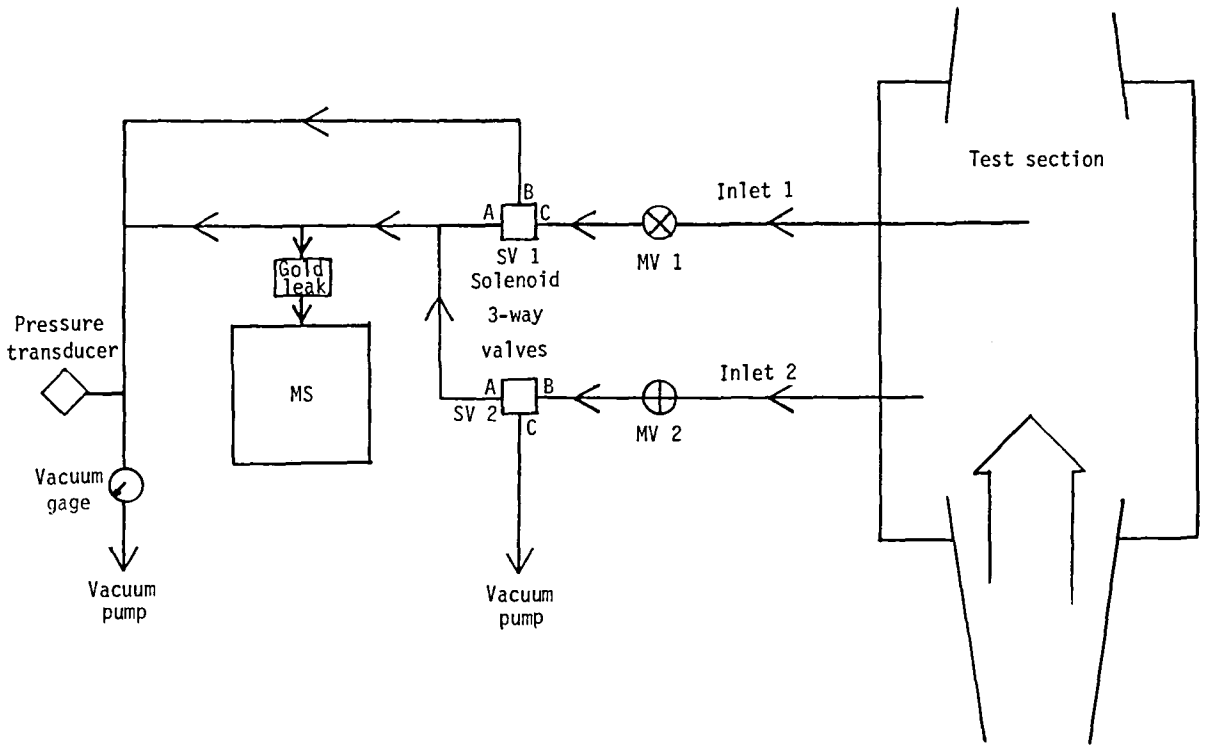

Figure 2. Schematic of mass spectrometric sampling system for tests in 7-Inch HTT.

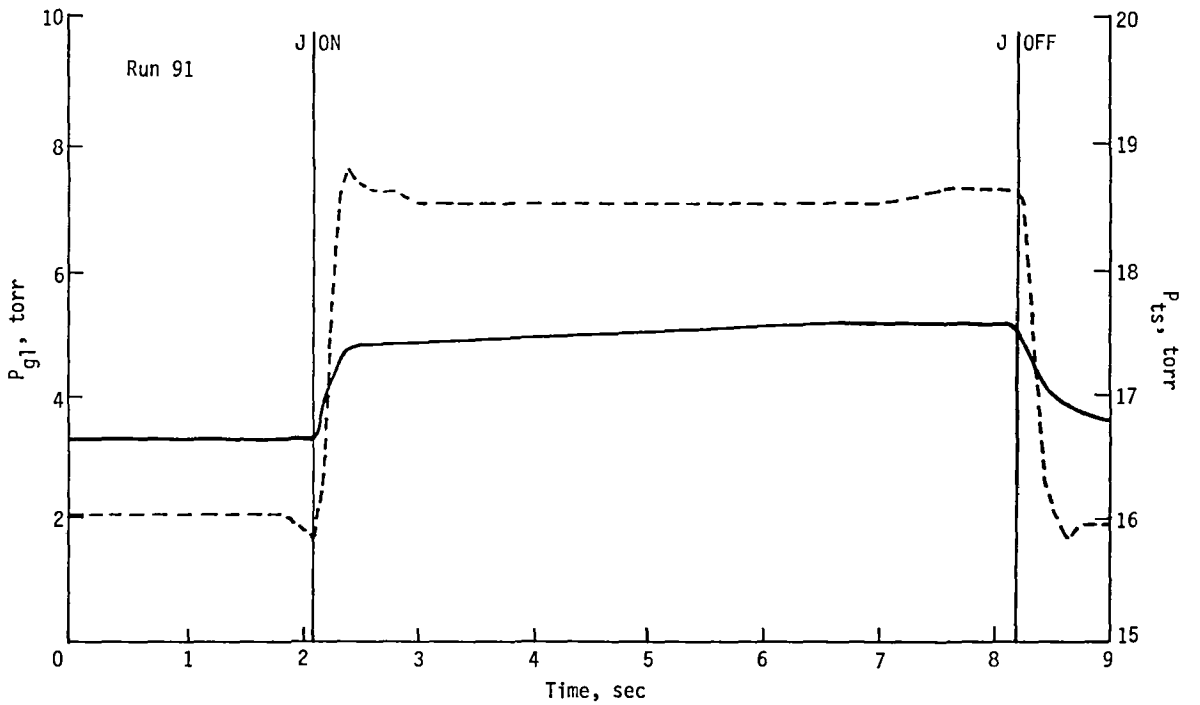

Figure 3. Pressure-time curves for a run where He jet was fired when model was below hot test stream.

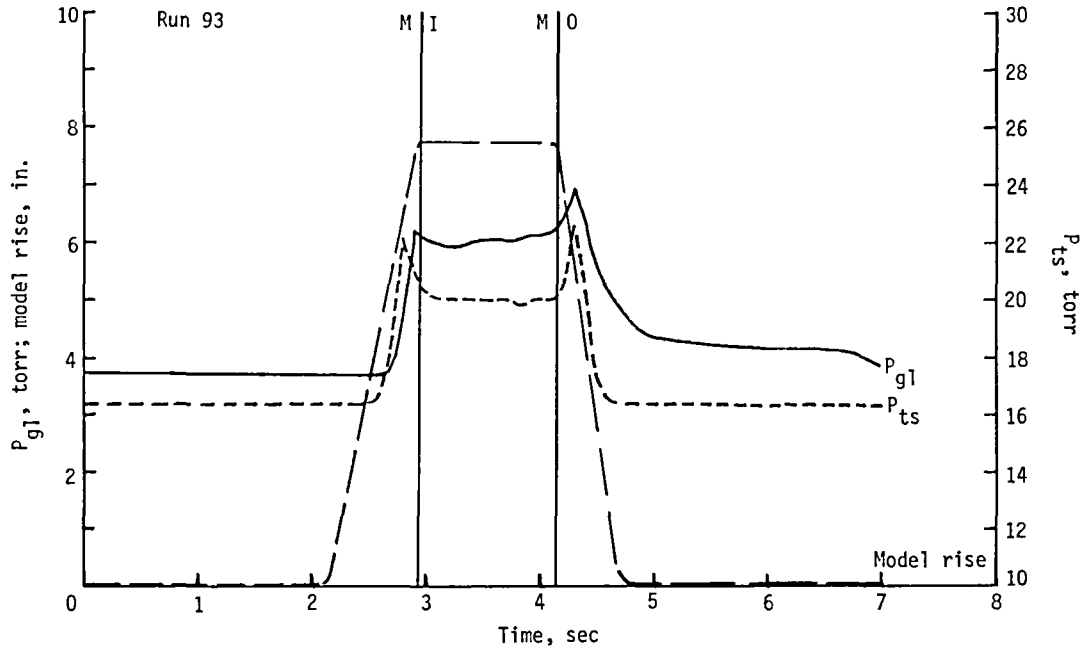

Figure 4. Pressure-time and model rise-time curves for a run where model was inserted into hot test stream but jet was not fired.

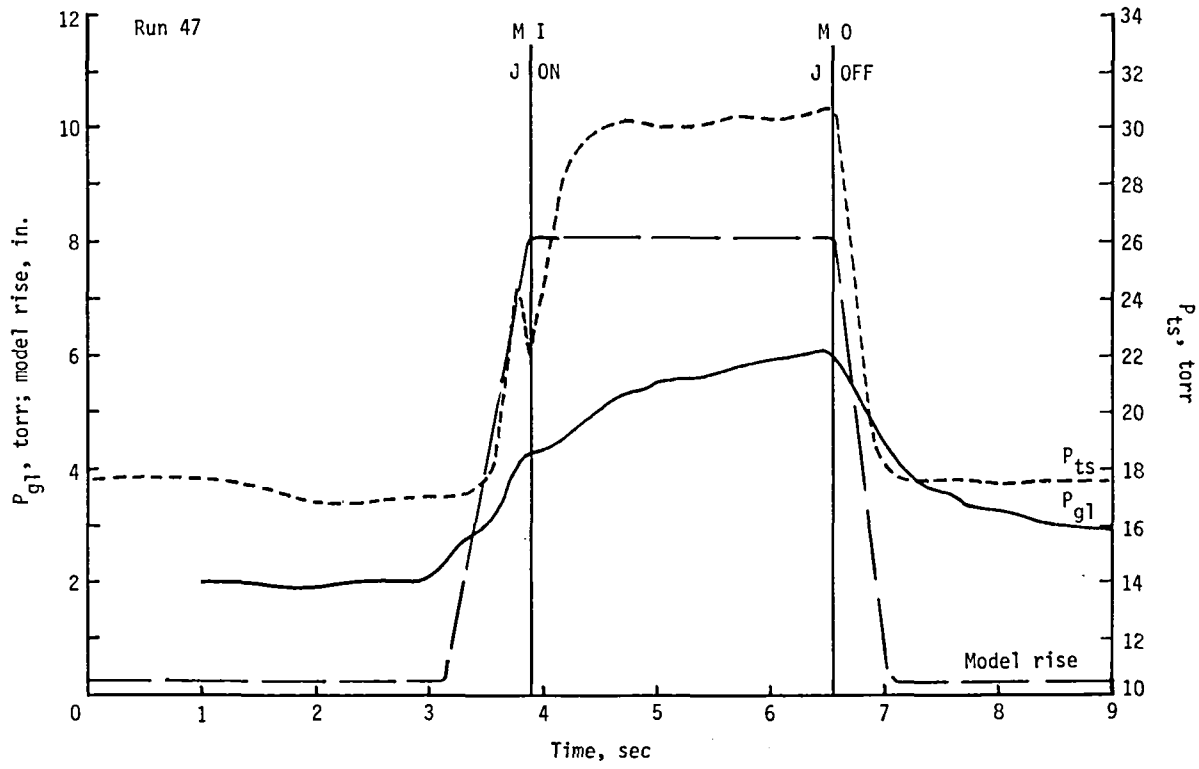

Figure 5. Pressure-time and model rise-time curves for a run where Ne/N_2 was injected into hot test stream.

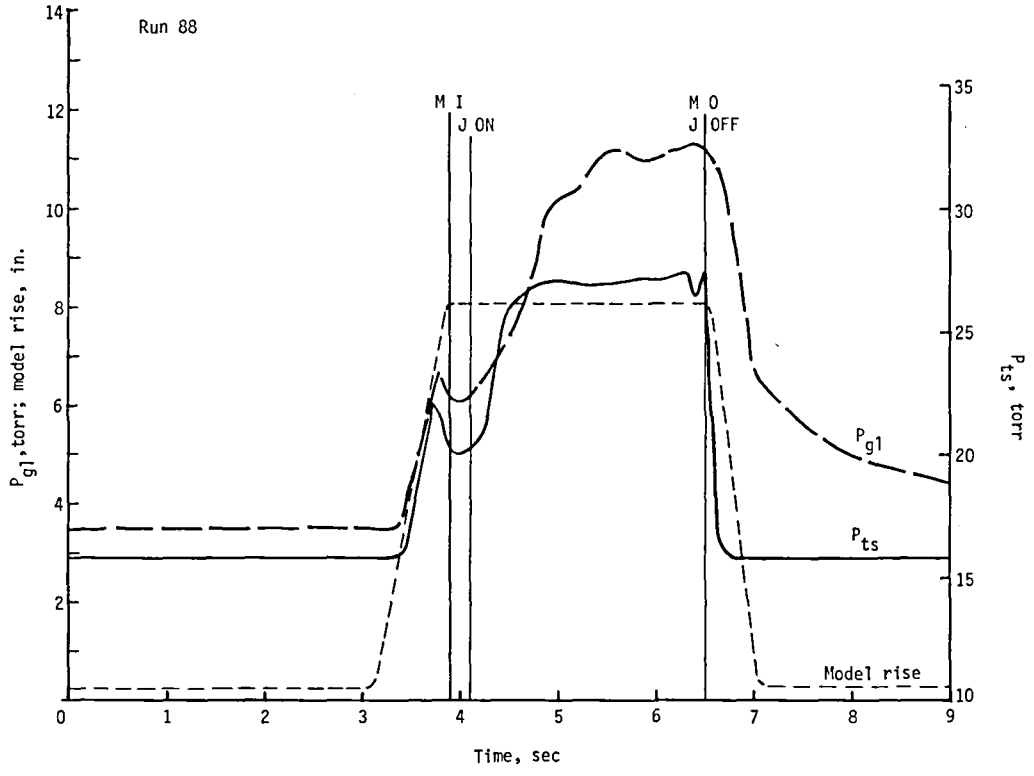

Figure 6. Pressure-time and model rise-time curves for a run where He was injected into hot test stream.

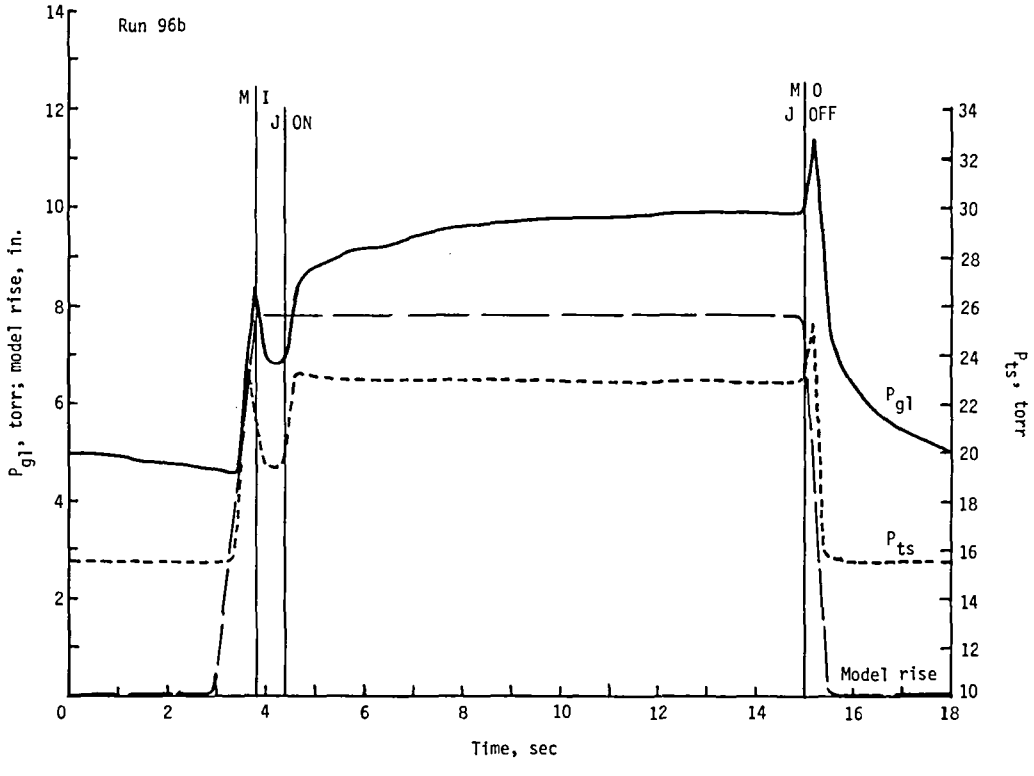

Figure 7. Pressure-time and model rise-time curves for a run where He was injected into the cold test stream.

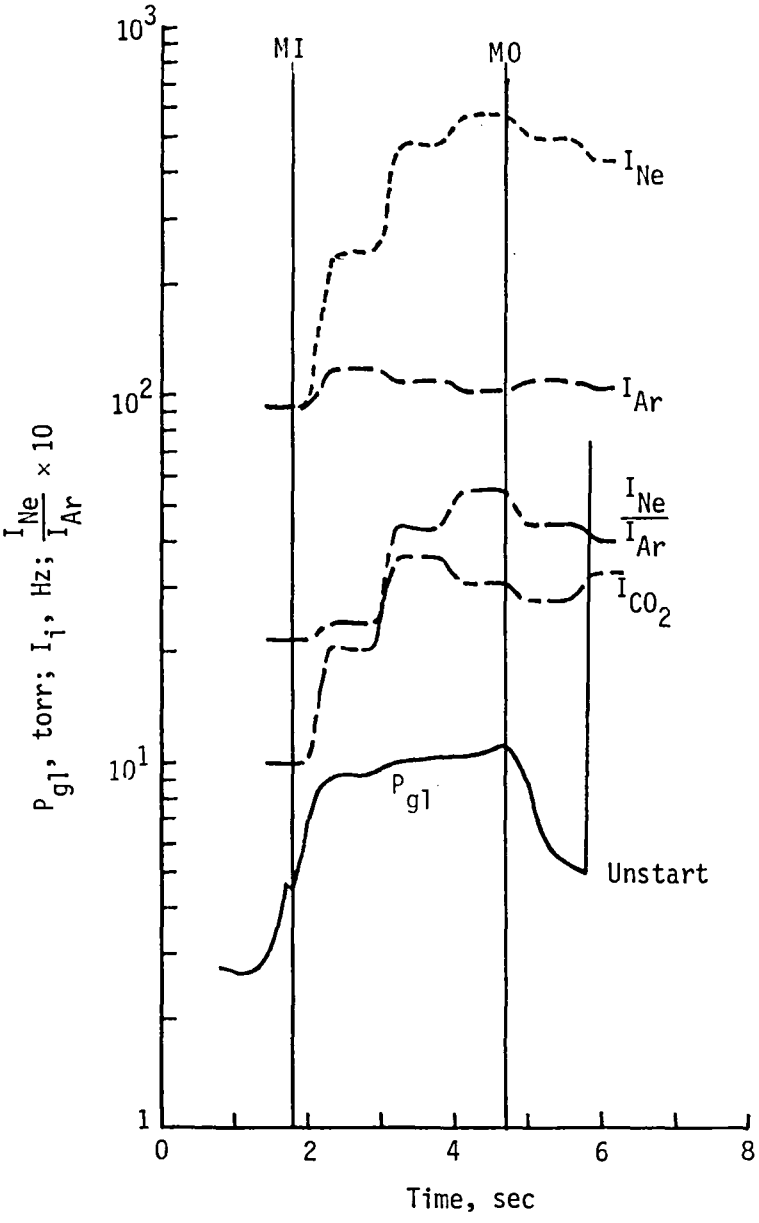

Figure 8. MS data for run 72 where Ne/N_2 was injected into a hot test stream and an unstart occurred soon after model withdrawal. I_{Ne}/I_{Ar} for complete mixing is 0.50.

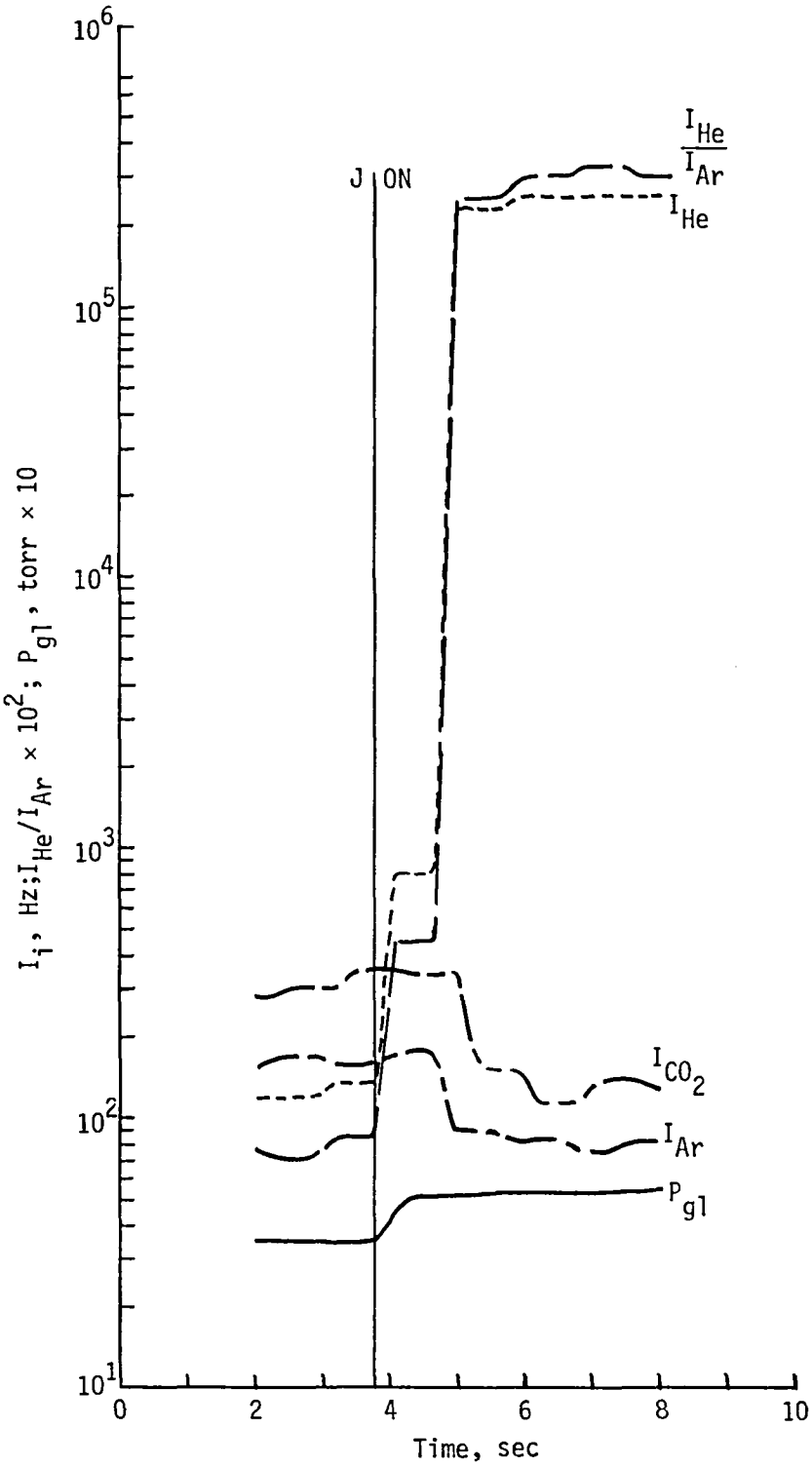

Figure 9. MS data for run 91 where He was ejected when model was below hot test stream.

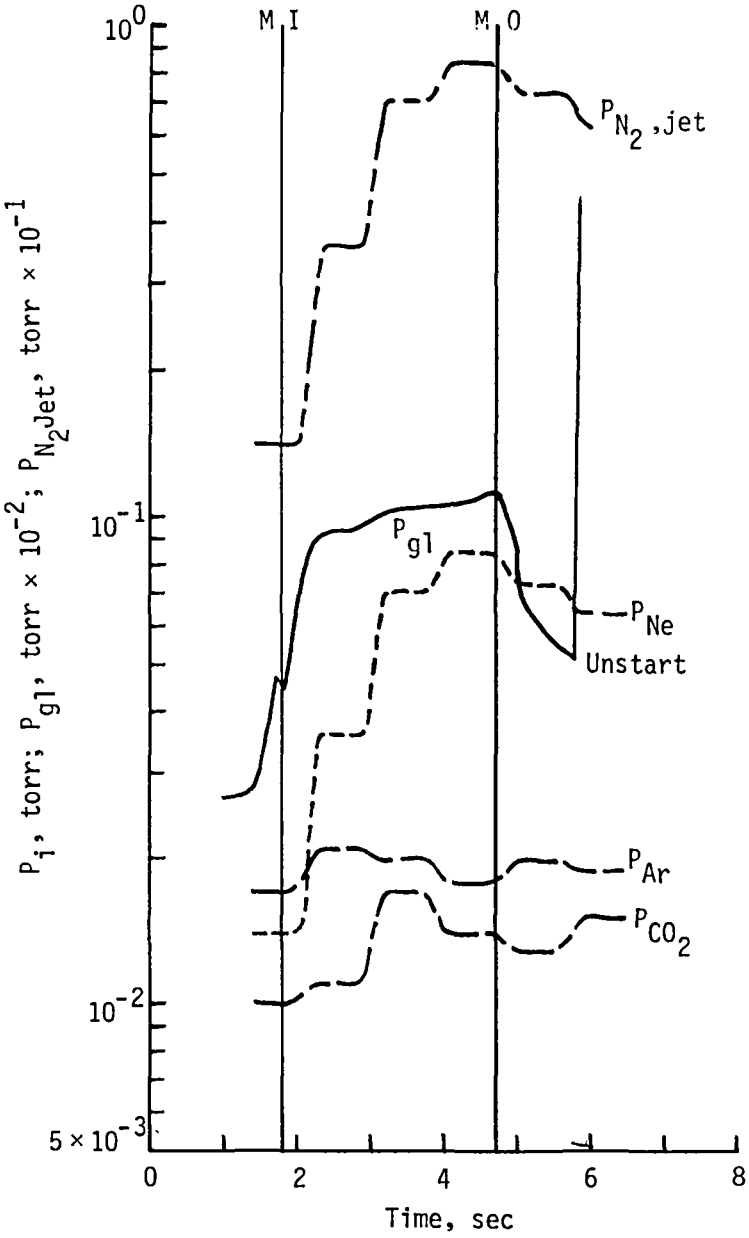

Figure 10. Partial pressures derived from MS data for run 72.

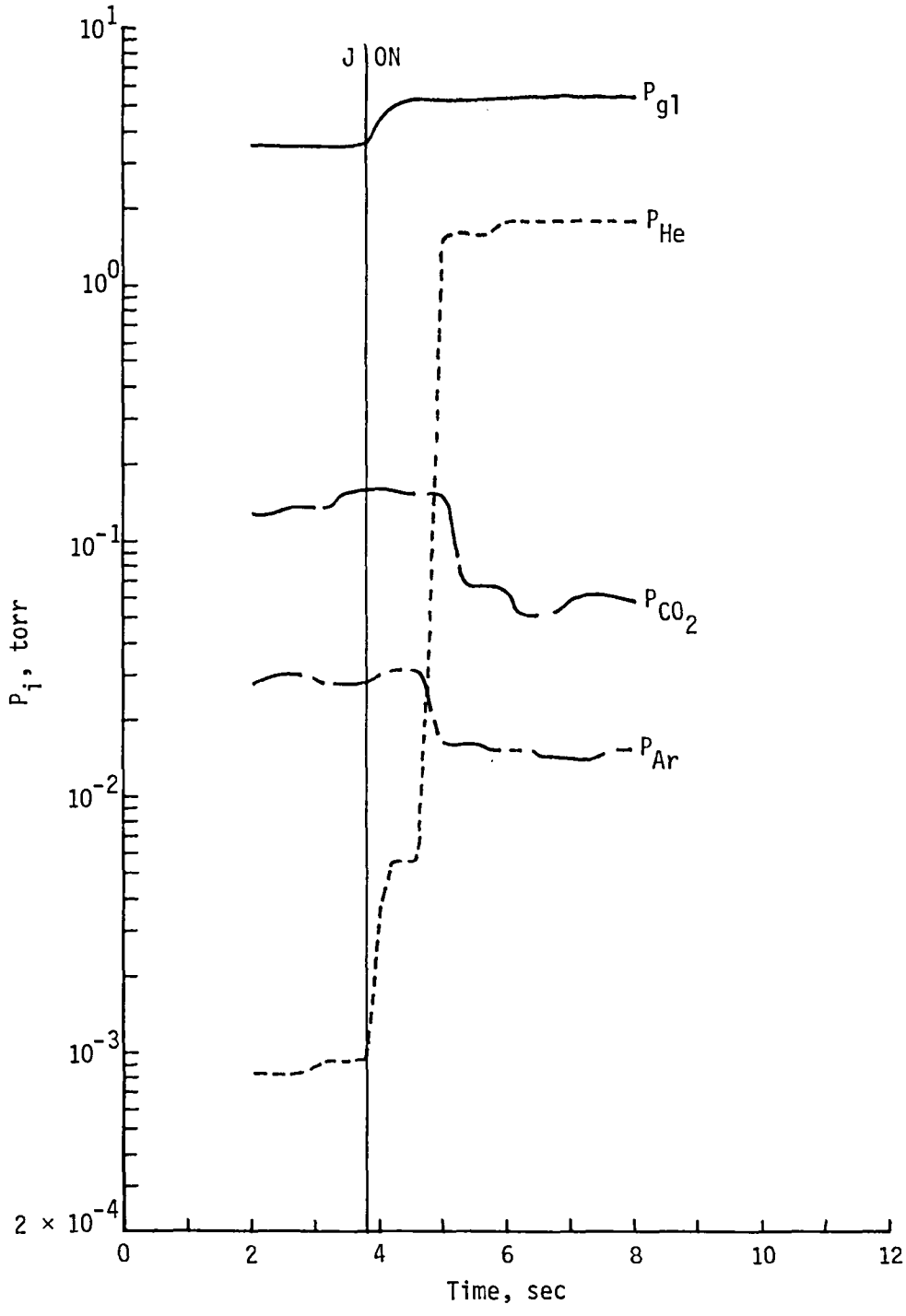

Figure 11. Partial pressures derived from MS data for run 91.

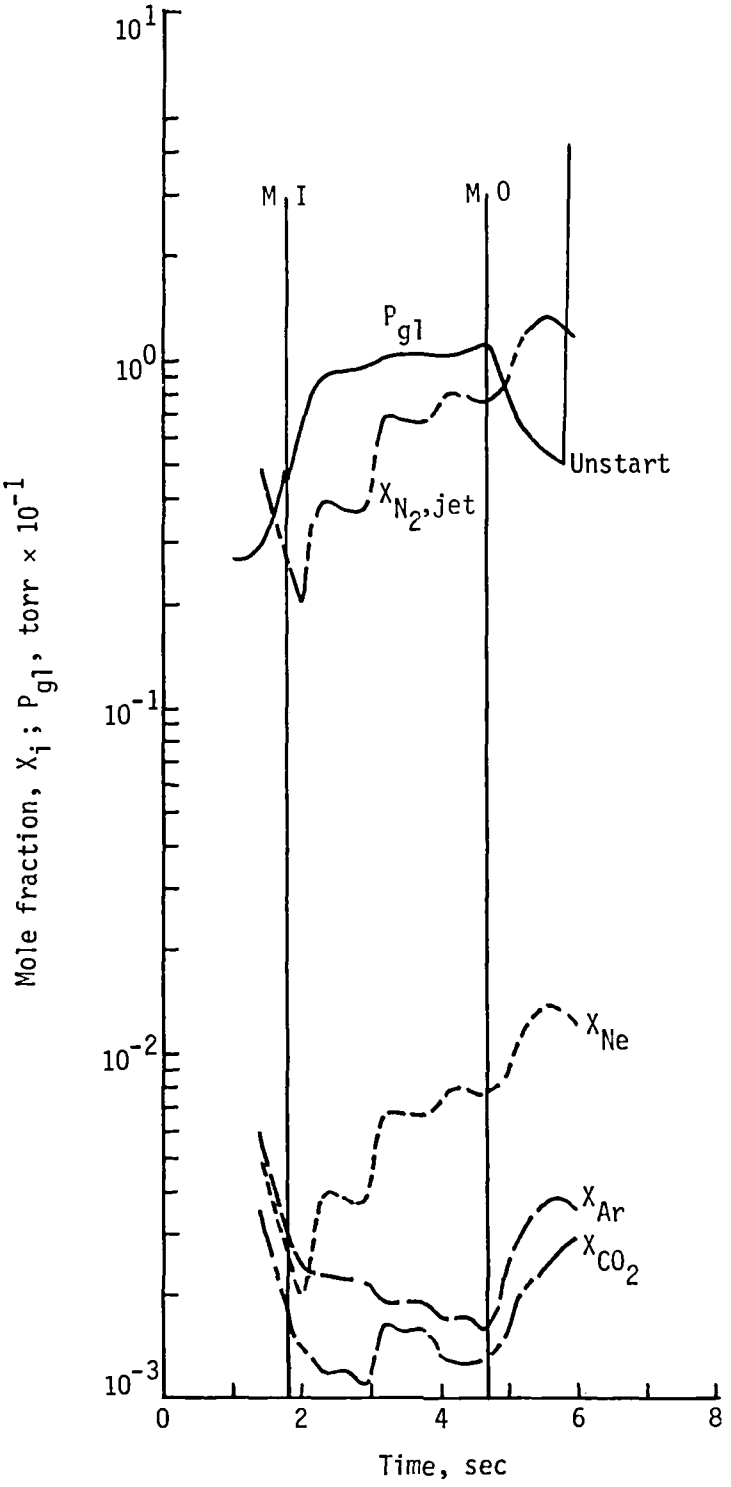

Figure 12. Mole fractions derived from MS data for run 72.

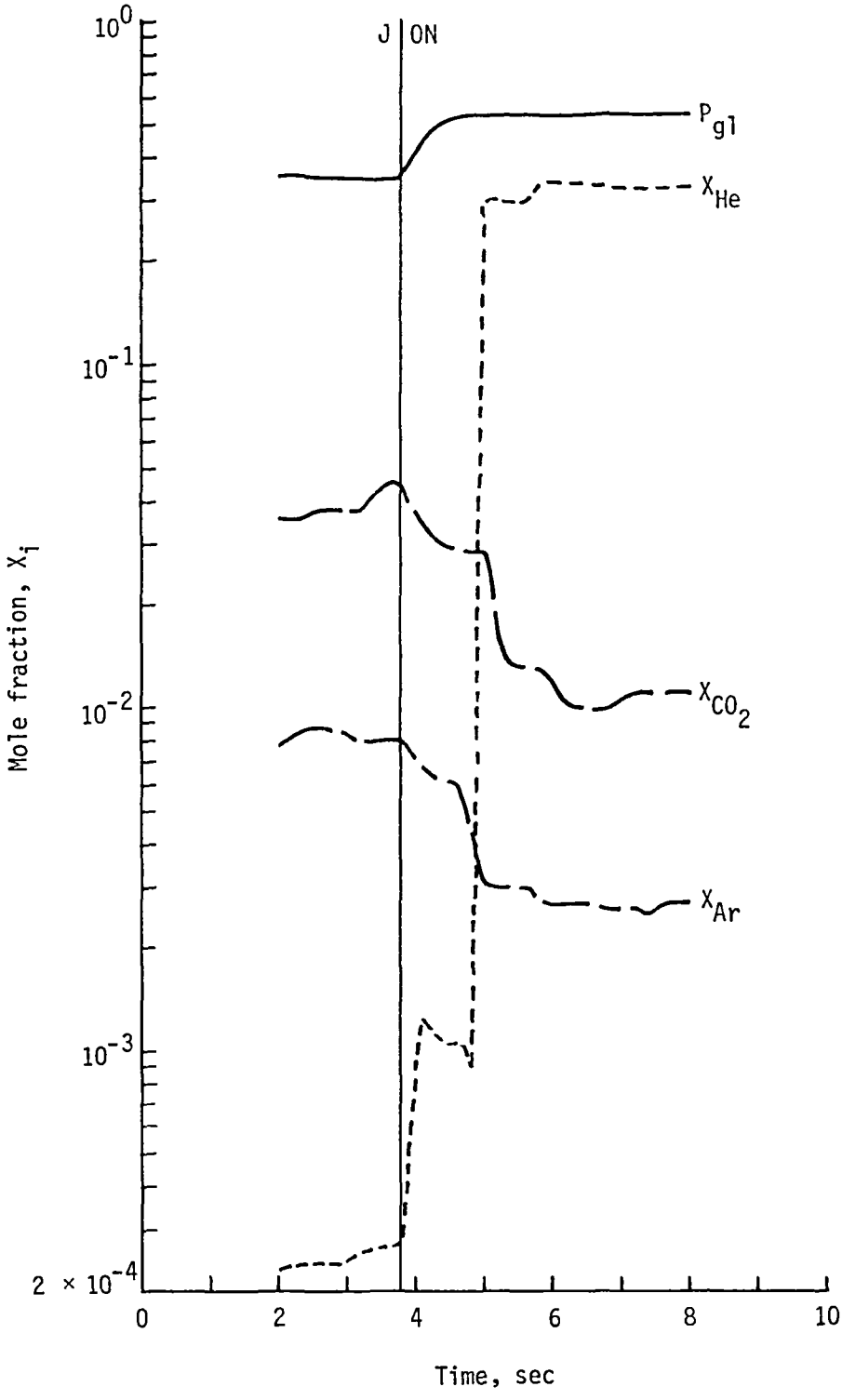

Figure 13. Mole fractions derived from MS data for run 91.

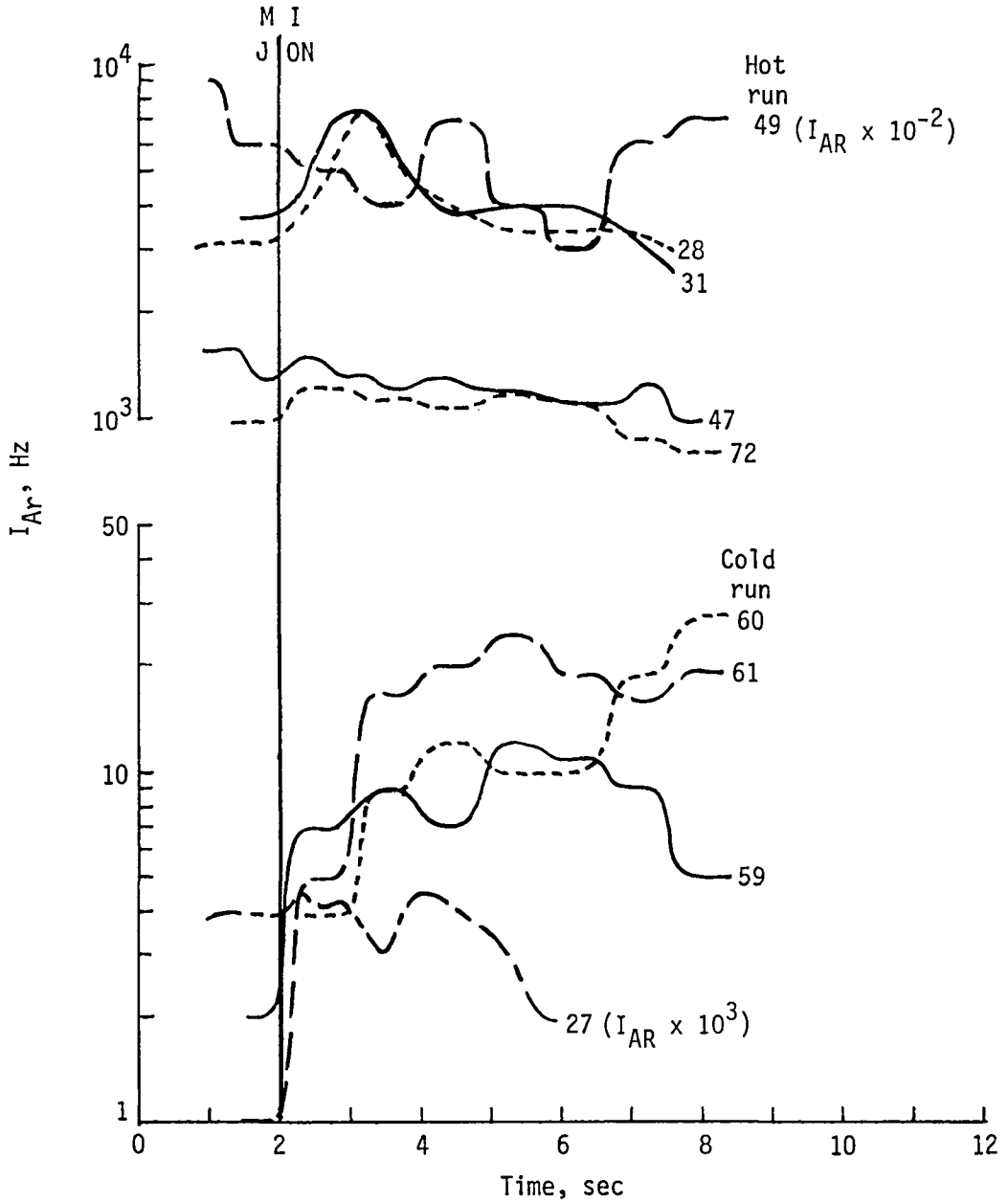

Figure 14. Comparison of Ar peak intensity data for runs where Ne/N_2 was injected into several hot or cold test streams. Run 27 is included where jet was ejected below a cold test stream.

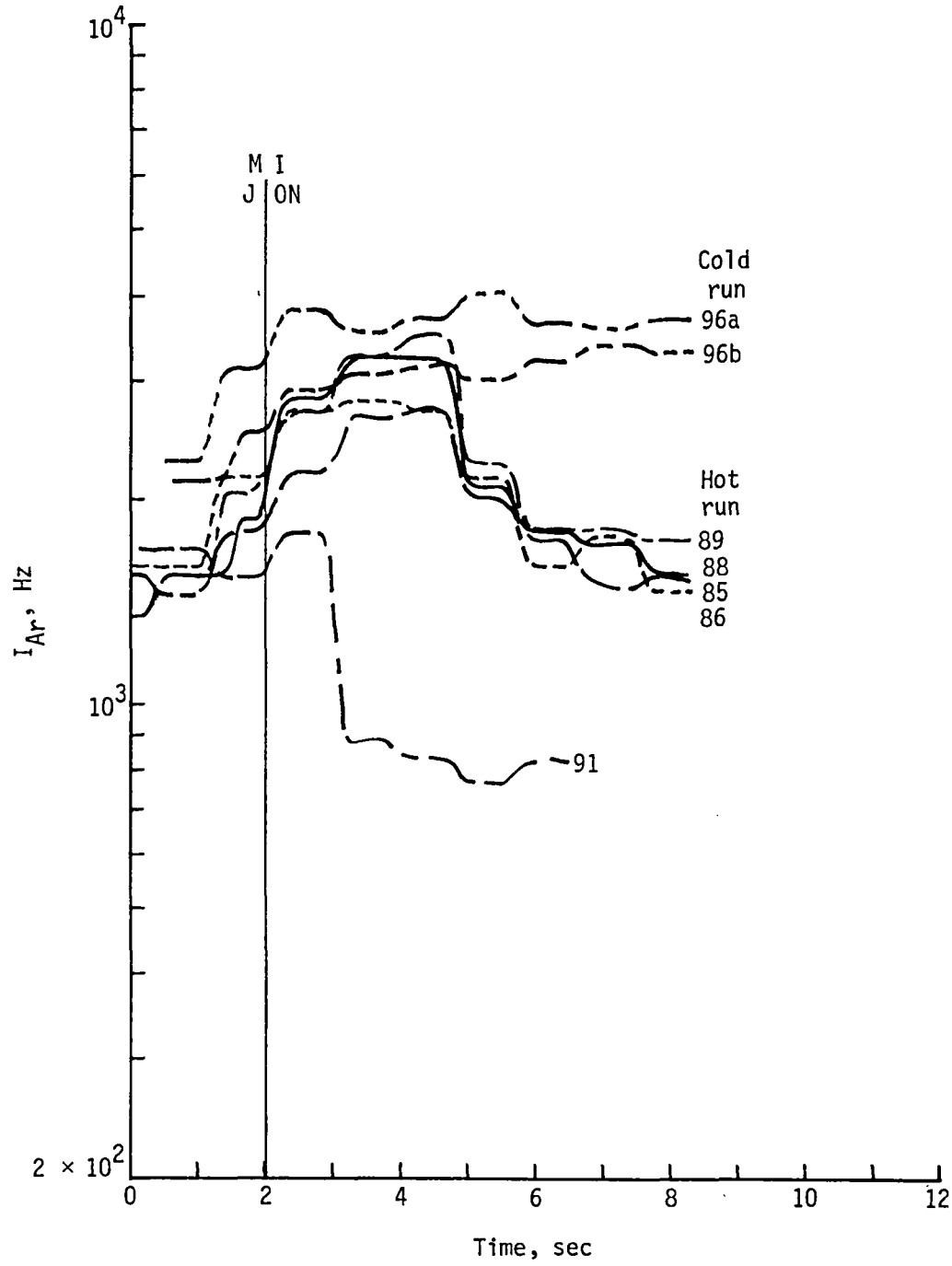

Figure 15. Comparison of Ar peak intensity data for runs where He was injected into several hot or cold test streams. Run 91 is included where jet was ejected below a hot test stream.

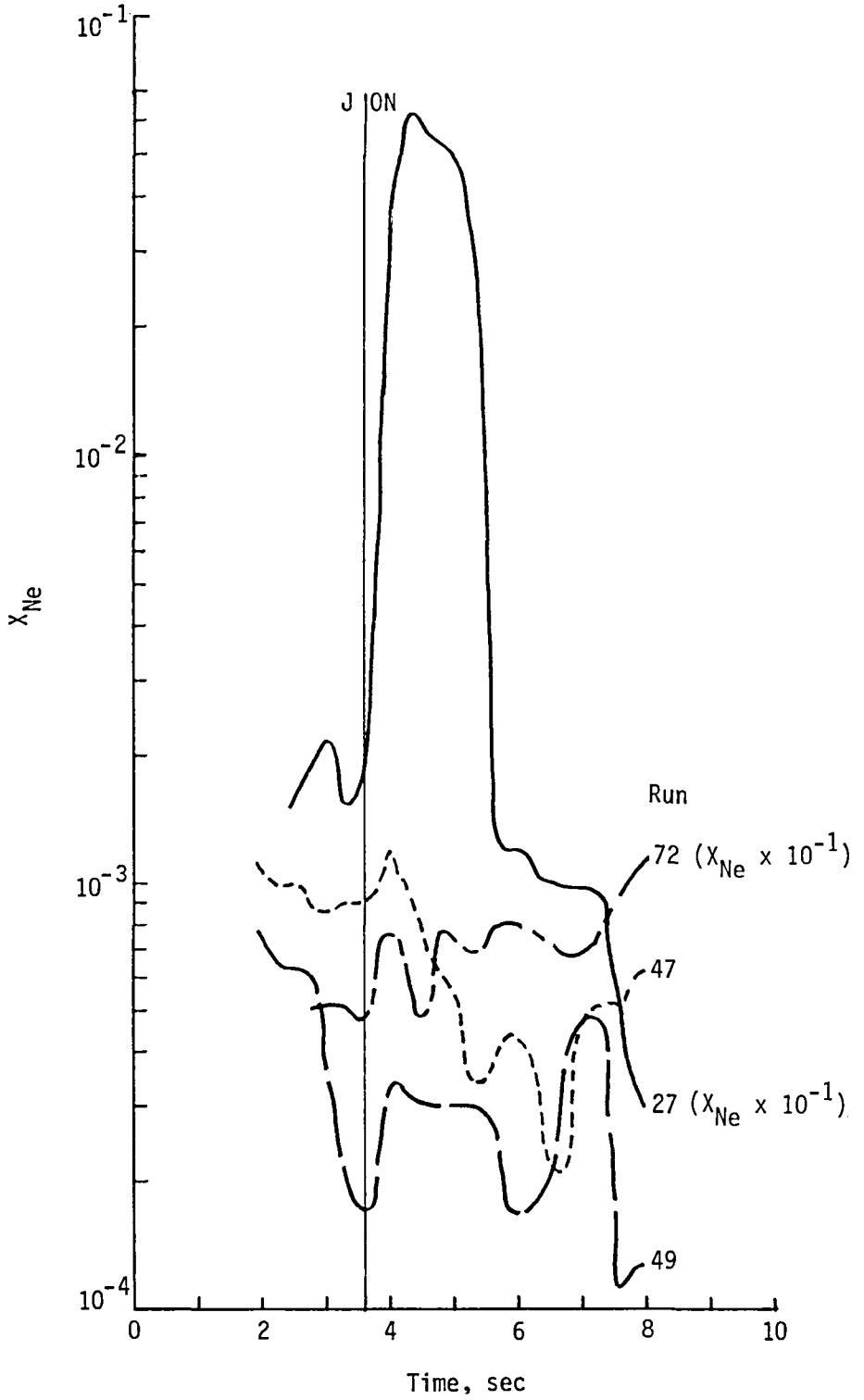

Figure 16. Comparison of Ne mole fraction data for several runs where 1 mole percent Ne/N_2 was injected into hot test streams. Run 27 is included where jet was ejected below a cold test stream.

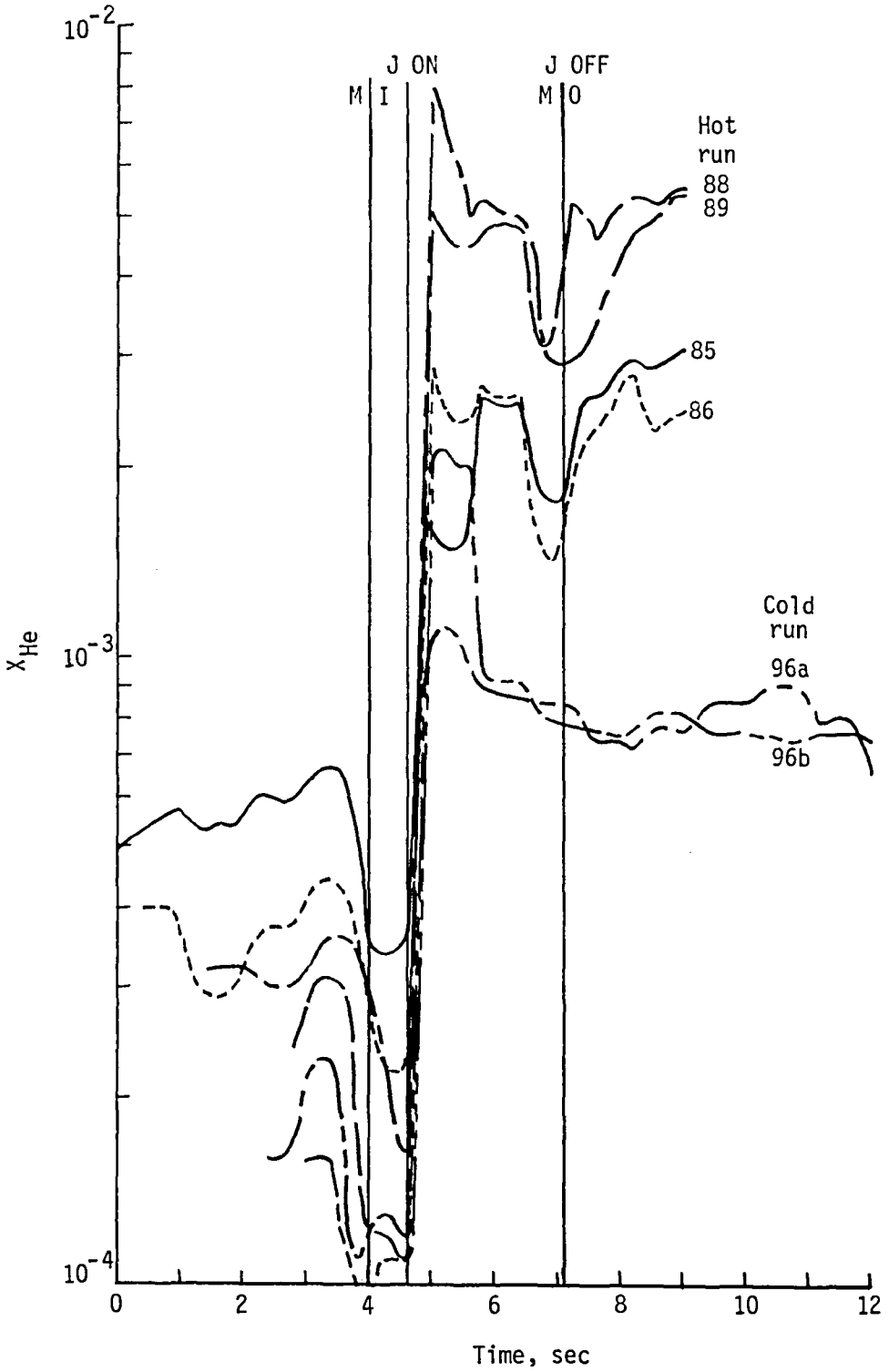

Figure 17. Comparison of He mole fraction data for several runs where He was injected into hot or cold test streams.

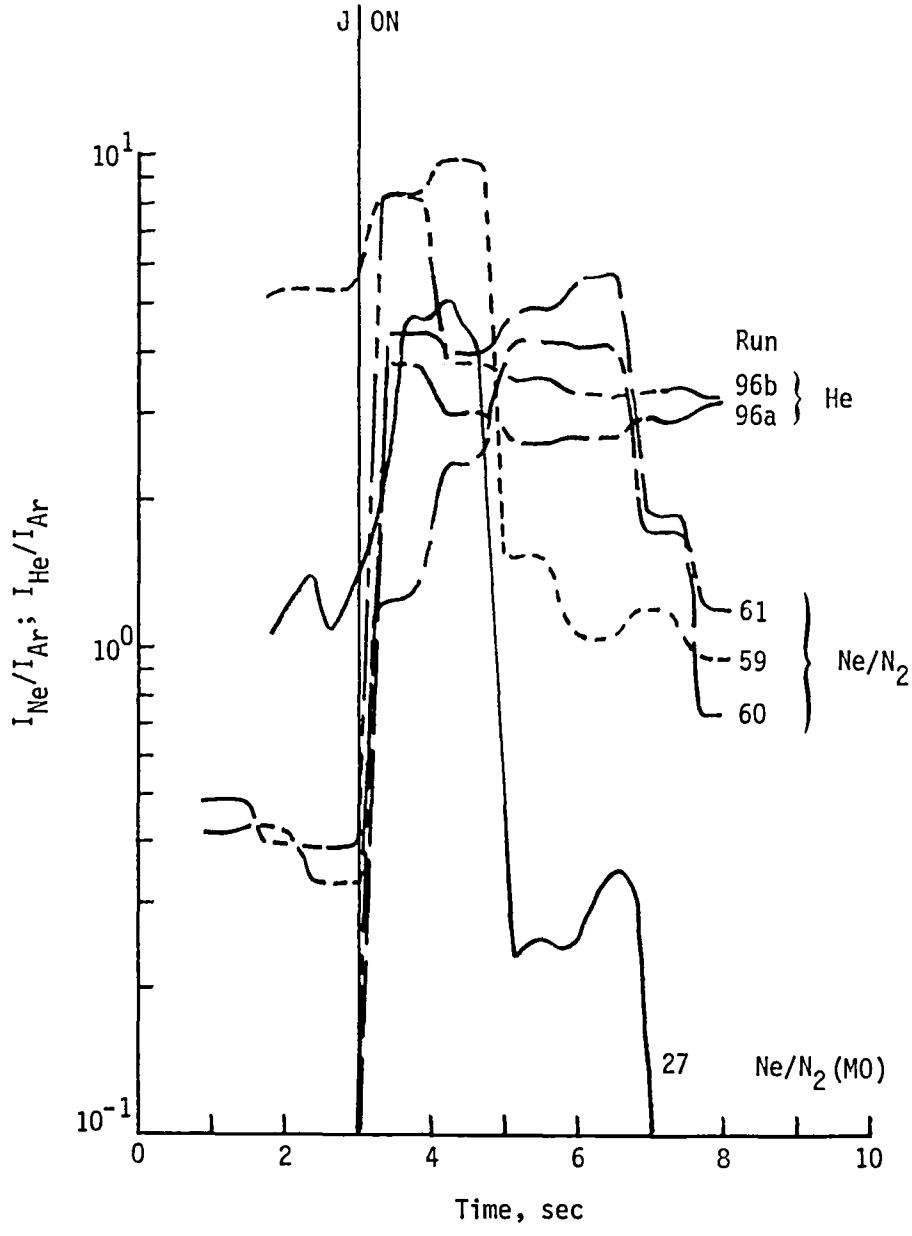

Figure 18. Comparison of intensity-ratio curves for several cold test-stream runs.

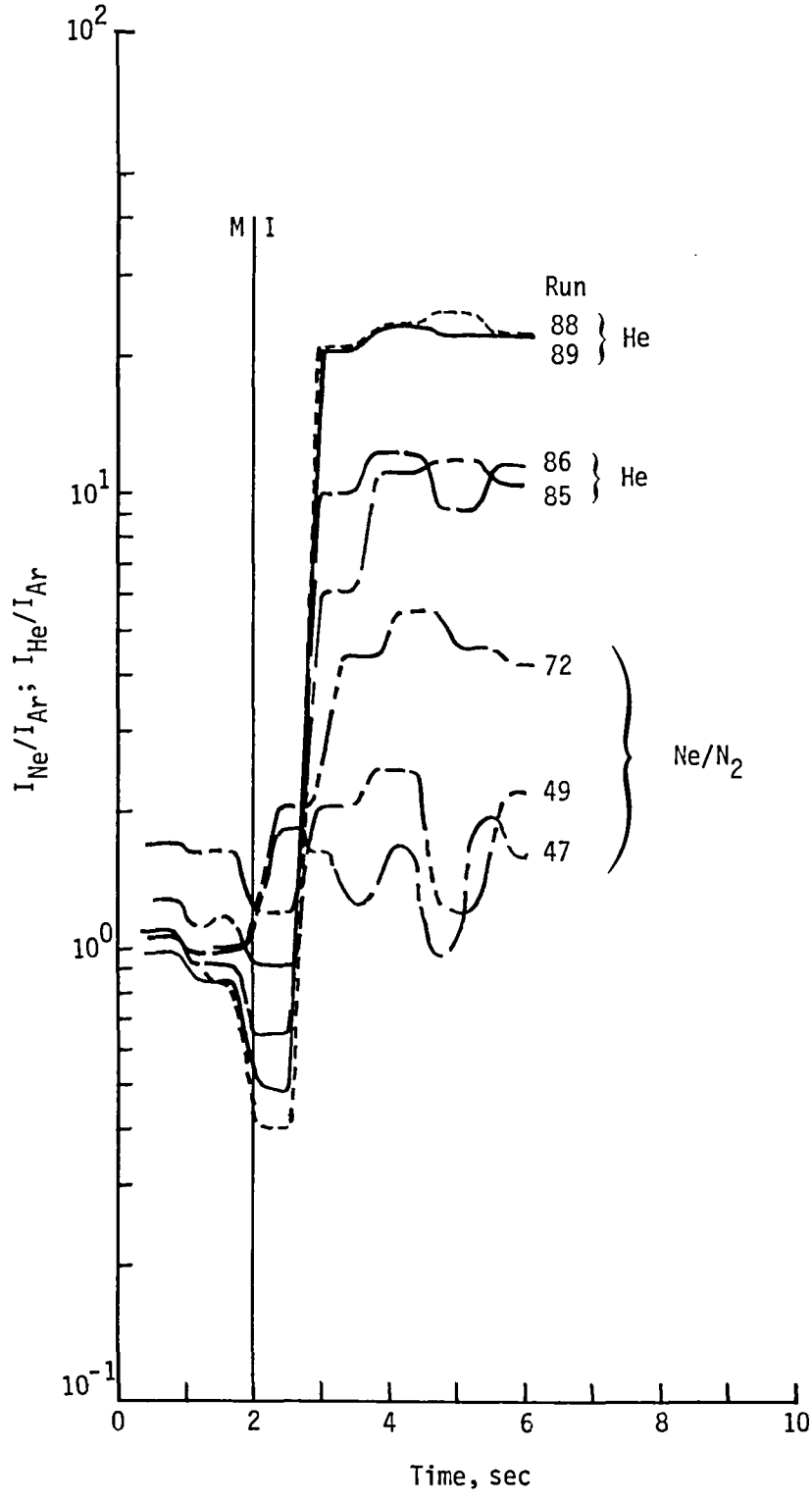

Figure 19. Comparison of intensity-ratio curves for several hot test-stream runs.

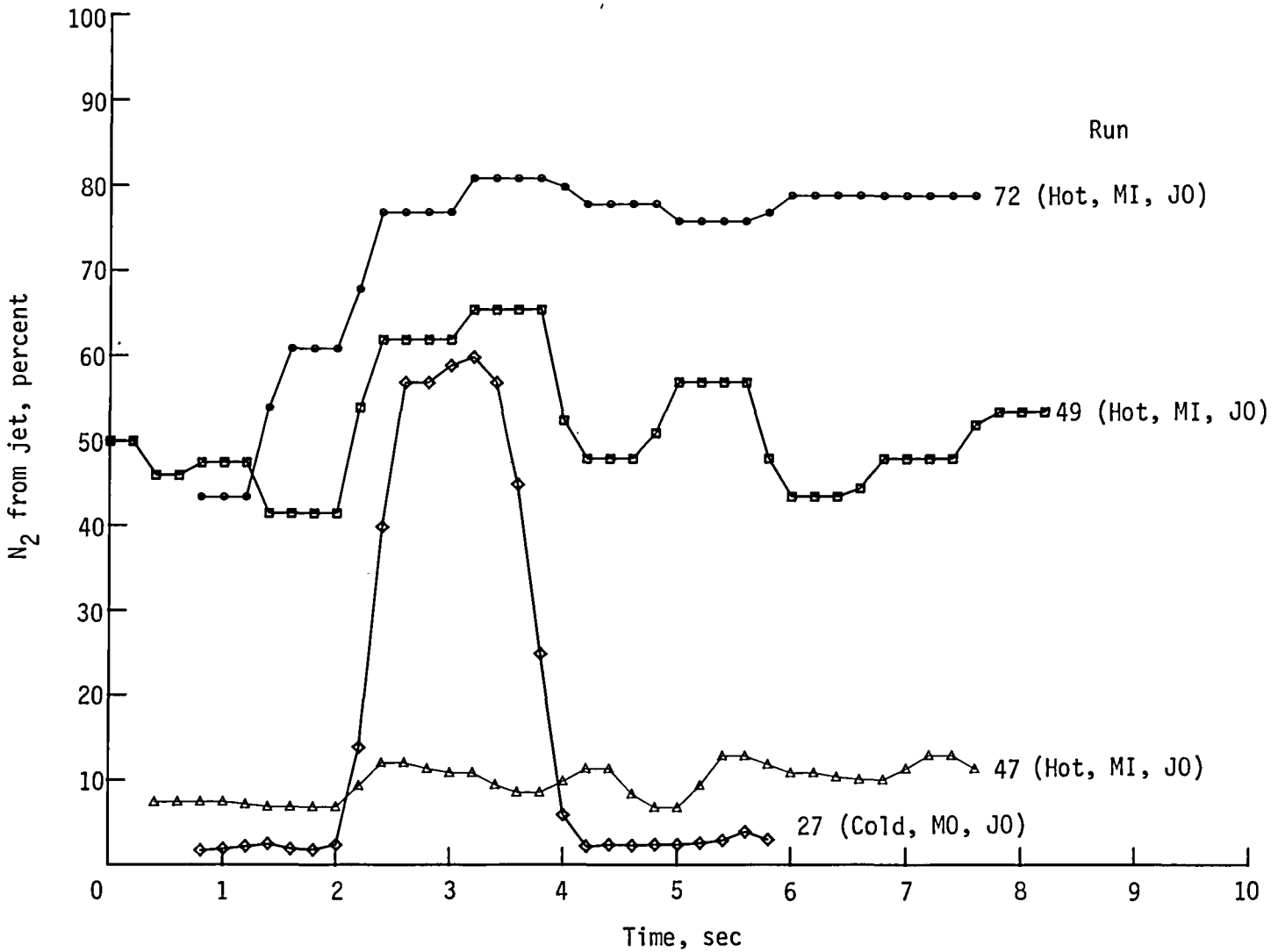

Figure 20. Mole percent N_2 from injected jet gas found in gas sampled at top of test section (ports A and B1) during several runs.

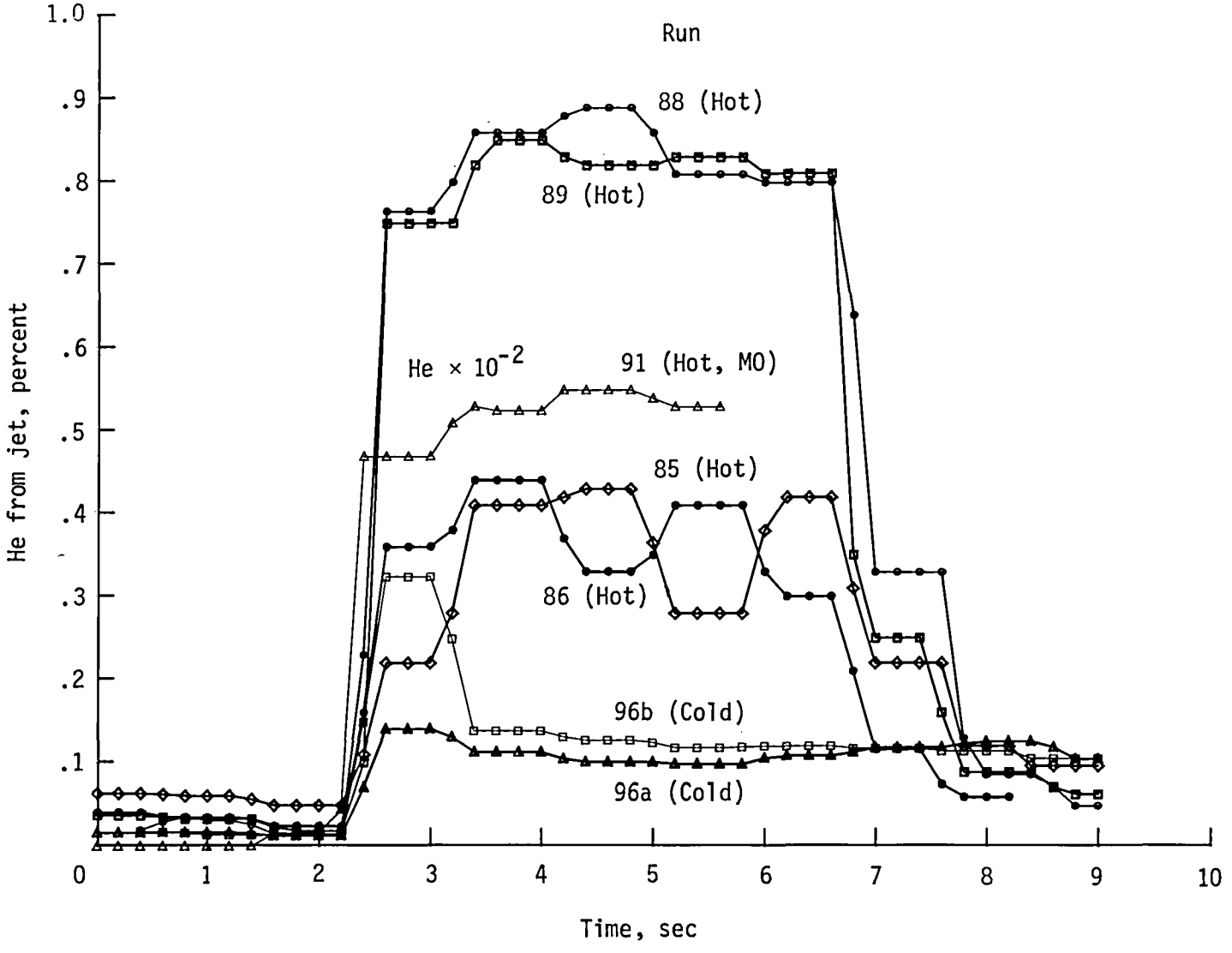

Figure 21. Mole percent He from ejected jet gas found in gas sampled at top of test section from several runs using several sample port positions. Note different scale for run 91.

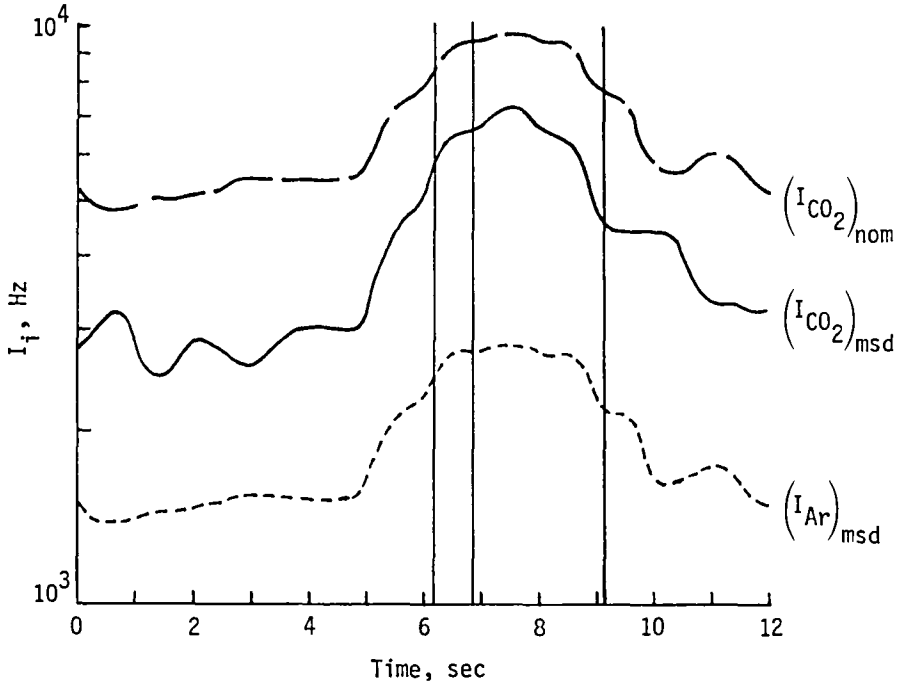

(a) Nominal and measured peak intensity curves.

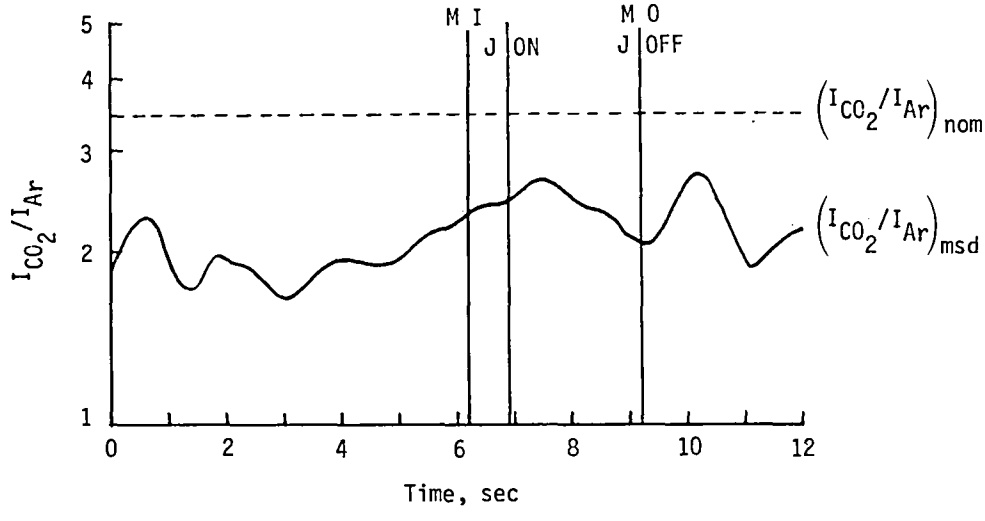

(b) Nominal and measured intensity ratios of CO_2 to Ar.

Figure 22. CO_2 and Ar data for run 86.

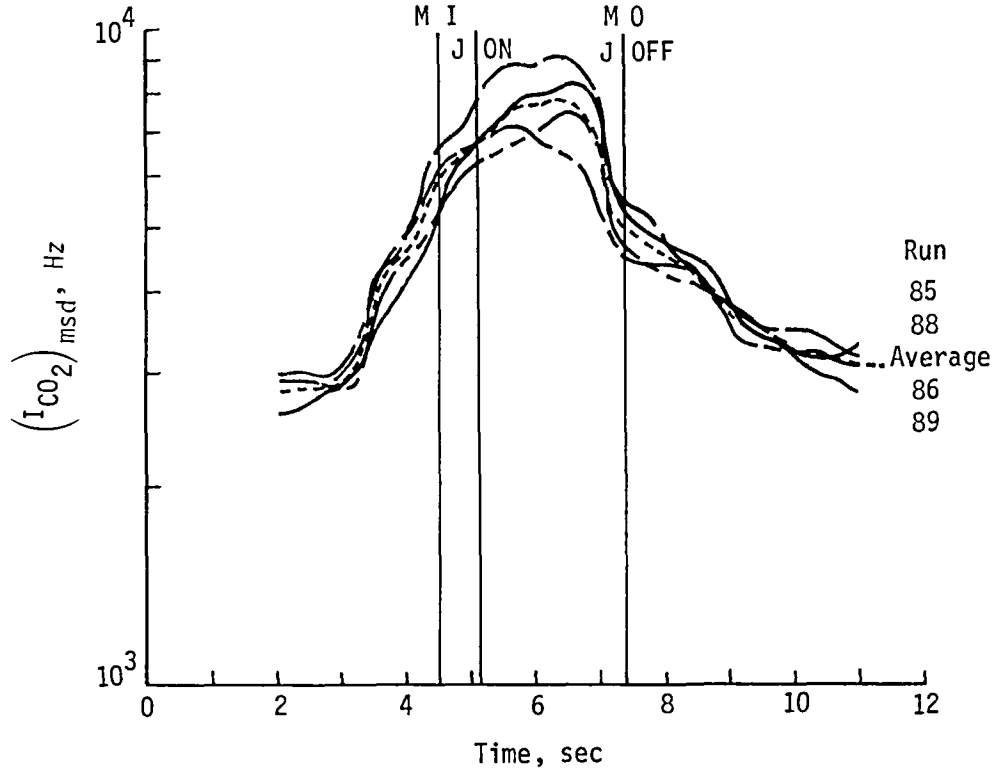

Figure 23. Measured peak intensity curves for CO_2 for runs 85, 86, 88, and 89 and their average.

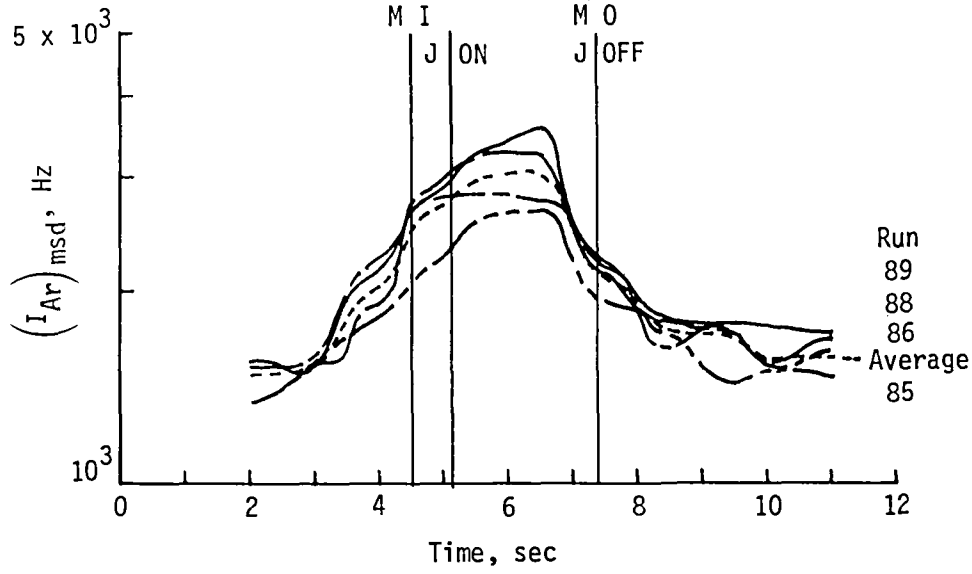

Figure 24. Measured peak intensity curves for Ar for runs 85, 86, 88, and 89 and their average.

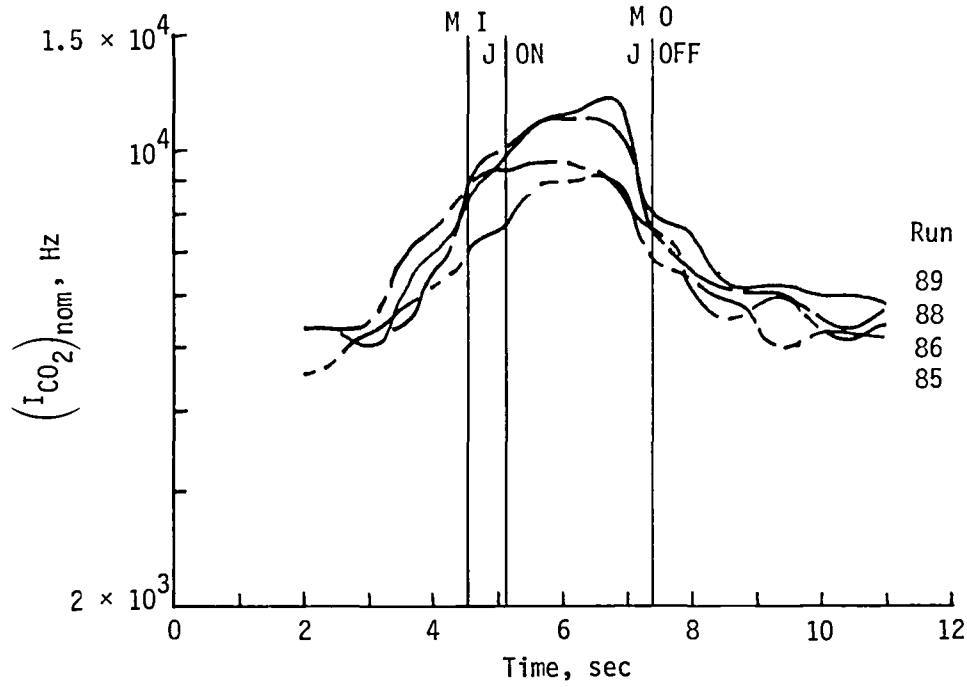

Figure 25. Nominal peak intensity curves for CO_2 for runs 85, 86, 88, and 89 calculated from known composition and measured I_{Ar}.

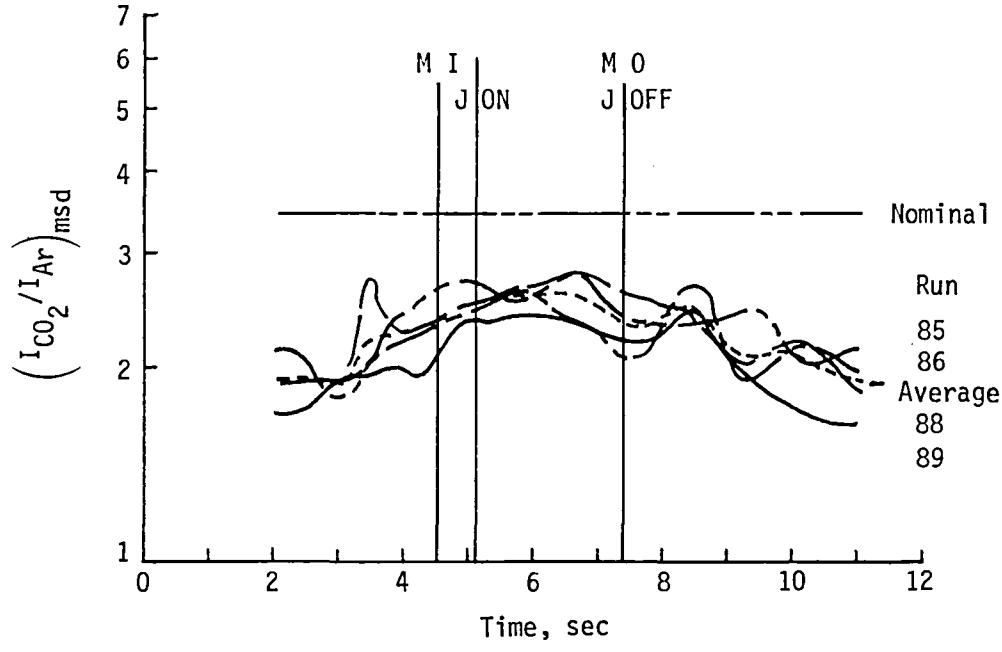

Figure 26. Nominal and measured peak intensity-ratio curves for runs 85, 86, 88, and 89 and average of measured ratios.

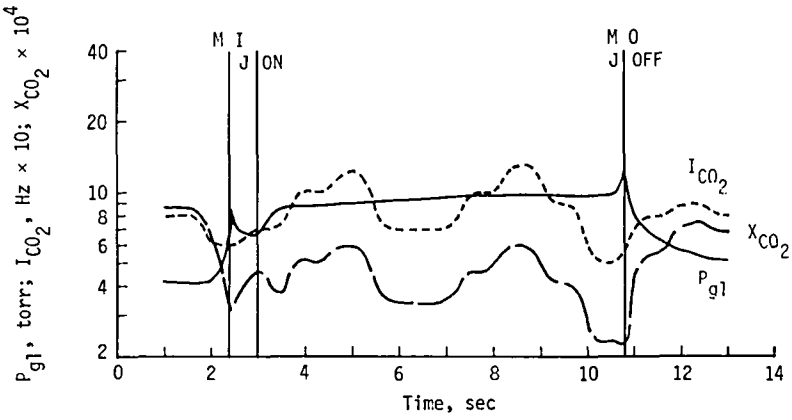

(a) Run 96a; cold; He jet injection.

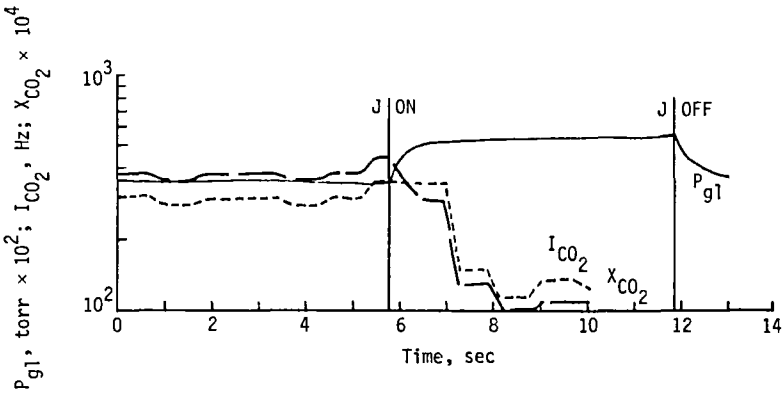

(b) Run 91; hot; He jet fired below test stream.

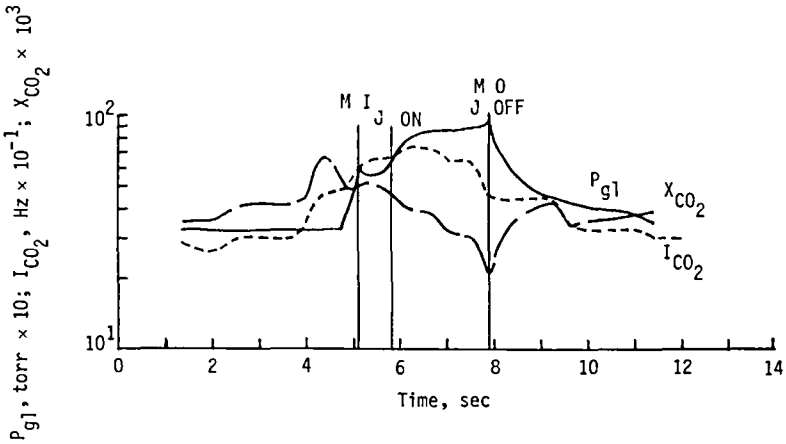

(c) Run 86; hot; He jet injection.

Figure 27. CO_2 and gold-leak pressure data for three types of runs.

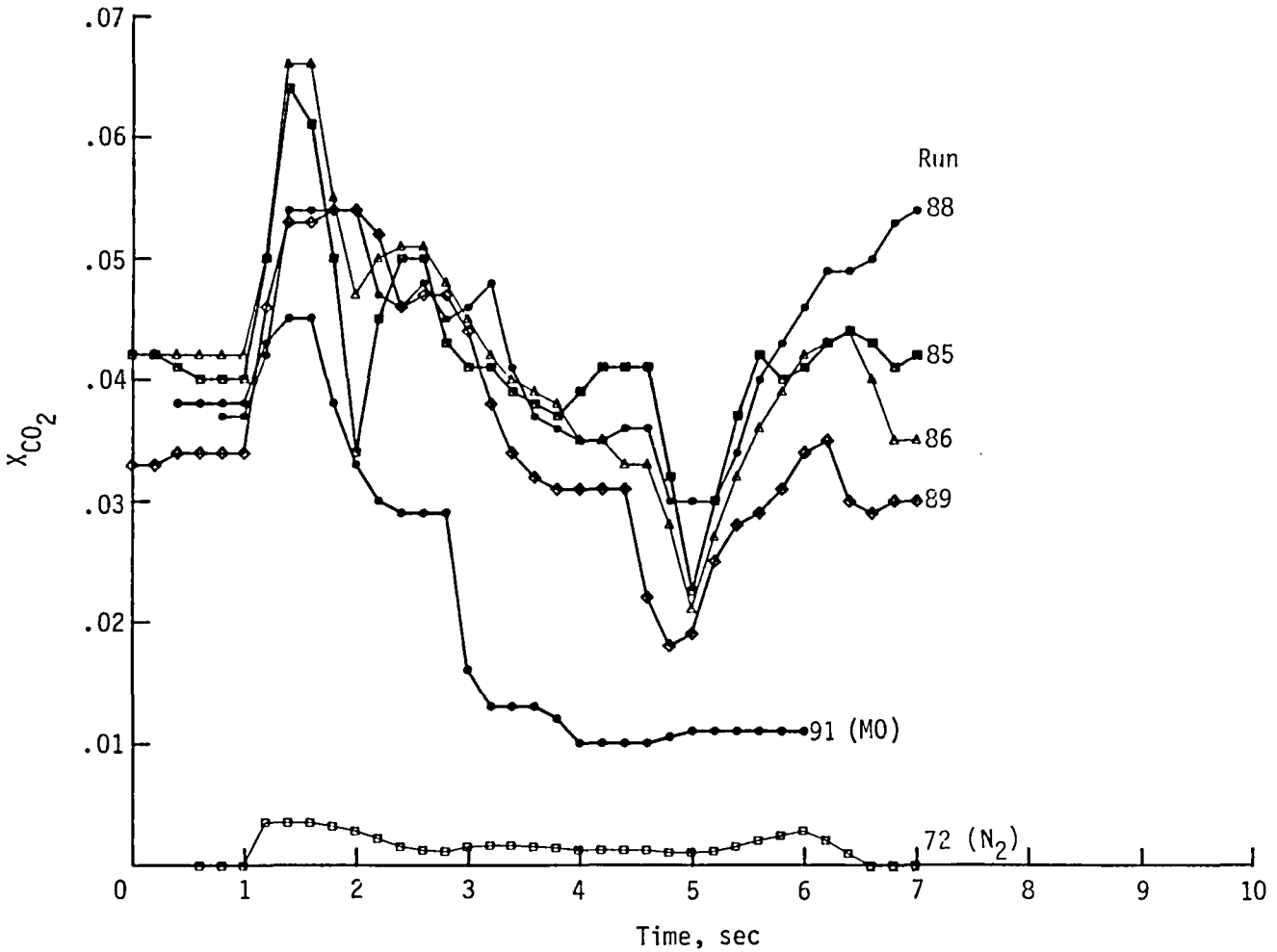

Figure 28. Mole fraction of CO_2, X_{CO_2} as a function of time for several hot test-stream runs with He jet gas and one with N_2 jet gas.

Standard Bibliographic Page

1. Report No.	2. Government Accession No.	3. Recipient's Catalog No.
NASA TM-87642		

4. Title and Subtitle	5. Report Date
Mass Spectrometric Gas Composition Measurements Associated With Jet Interaction Tests in a High-Enthalpy Wind Tunnel	June 1986
	6. Performing Organization Code: 506-51-13-02
7. Author(s): Beverley W. Lewis, Kenneth G. Brown, George M. Wood, Jr., Richard L. Puster, Patricia A. Paulin, Charles E. Fishel, and D. Alan Ellerbe	8. Performing Organization Report No.: L-16074
9. Performing Organization Name and Address: NASA Langley Research Center, Hampton, VA 23665-5225	10. Work Unit No.
	11. Contract or Grant No.
12. Sponsoring Agency Name and Address: National Aeronautics and Space Administration, Washington, DC 20546-0001	13. Type of Report and Period Covered: Technical Memorandum
	14. Sponsoring Agency Code

15. Supplementary Notes

Beverley W. Lewis, George M. Wood, Jr., Richard L. Puster, Patricia A. Paulin, and D. Alan Ellerbe: Langley Research Center, Hampton, Virginia.
Kenneth G. Brown and Charles E. Fishel: Old Dominion University, Norfolk, Virginia.

16. Abstract

Knowledge of test gas composition is important in wind-tunnel experiments measuring aerothermodynamic interactions. This paper describes measurements made by sampling the top of the test section during runs of the Langley 7-Inch High-Temperature Tunnel. The tests were conducted to determine the mixing of gas injected from a flat-plate model into a combustion-heated hypervelocity test stream and to monitor the CO_2 produced in the combustion. The Mass Spectrometric (MS) measurements yield the mole fraction of N_2 or He and CO_2 reaching the sample inlets. The data obtained for several tunnel run conditions are related to the pressures measured in the tunnel test section and at the MS ionizer inlet. The apparent distributions of injected gas species and tunnel gas (CO_2) are discussed relative to the sampling techniques. The measurements provided significant real-time data for the distribution of injected gases in the test section. The jet N_2 diffused readily from the test stream, but the jet He was mostly entrained. The amounts of CO_2 and Ar diffusing upward in the test section for several run conditions indicated the variability of the combustion-gas test-stream composition.

17. Key Words (Suggested by Authors(s))	18. Distribution Statement
Mass spectrometry Gas composition High enthalpy Sampling Wind tunnel	Unclassified—Unlimited Subject Category 25

19. Security Classif.(of this report)	20. Security Classif.(of this page)	21. No. of Pages	22. Price
Unclassified	Unclassified	31	A03

For sale by the National Technical Information Service, Springfield, Virginia 22161

NASA-Langley, 1986

National Aeronautics and
Space Administration
Code NIT-4

Washington, D.C.
20546-0001

Official Business
Penalty for Private Use, $300

BULK RATE
POSTAGE & FEES PAID
NASA
Permit No. G-27

POSTMASTER: If Undeliverable (Section 158 Postal Manual) Do Not Return